Nonlinear state observers for robots with elastic joints

A. Caciolai, P. Pustina

July 22, 2020

Contents

1 Introduction

The problem of estimating the full state of an elastic joint robot is a longstanding problem in the literature, since the control of this kind of robots through static state feedback requires the knowledge of the four state variables for each joint, usually joints and motors positions and their time derivatives [1]. In this context, in our project we implemented and compared two different observers whose state estimate is exploited to control a manipulator with two different controllers.
This report is structured as follows:

- In Section 2 we outline the derivation of the dynamic model of an elastic joint robot we used, following [1] [2];
- In Section 3 we describe the observers employed;

- In Section 4 we describe the controllers employed;
- In Section 5 we report the results of the simulation of various scenarios.

2 Modelling

As anticipated in the introduction, the modelling reflects closely the models introduced by [1] and [2], which are very similar but present slight differences due to different starting assumptions. This will be clarified in the following.
Consider a manipulator consisting of n rigid links interconnected by n elastic joints. It is assumed for simplicity that the joints are of the *revolute* type and that elasticity is modelled as a linear torsional spring, with stiffness k_i. The presence of elasticity at the level of the joints implies that the transmission between each link and its motor is not perfectly rigid, but instead, there is an elastic coupling between the motor shaft attached to the rotor and the link. Since the position of the rotors is not identically equal to the position of the links during the motion of the manipulator, elasticity introduces an additional degree of freedom for each joint, thus the manipulator can be modelled as a $2n$-dof system.

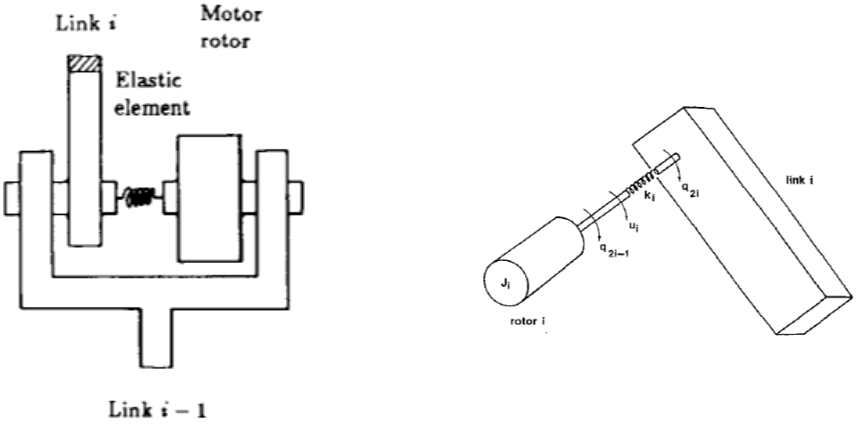

Figure 1: Possible schemes of an elastic joint.

Therefore, let $\mathbf{q} = (q_1, \ldots, q_{2n})^\top$ be a set of generalized coordinates for the system, with the following convention:

$$q_{2i} = \text{position of link } i \tag{2.1}$$

$$q_{2i-1} = \frac{1}{rg_i}\theta_i = \text{position of motor } i \text{ after the reduction,} \tag{2.2}$$

with θ_i the position of rotor i and rg_i the reduction gear ratio between motor i and link i, for $i = 1, \ldots, n$. We can compactly represent the coordinates as $\mathbf{q} = \left(\mathbf{q}_1^\top, \mathbf{q}_2^\top\right)^\top$, with $\mathbf{q}_1$ denoting the $n \times 1$ vector of link positions and $\mathbf{q}_2$ the $n \times 1$ vector of motor positions.

2.1 Assumptions

In the following derivation, it is assumed that:

1. The rotors are uniform bodies of rotation, so that we may establish the coordinate frame at their center of mass and assume that coordinate axes are principal axes, therefore having a diagonal inertia tensor;

2. Furthermore, the rotors kinetic energy is mainly due to their own rotation, so that their motion is a pure rotation with respect to an inertial frame, allowing to further simplify the expression of their kinetic energy;

3. Finally, the rotors are symmetric about their axis of rotation, so that the position of their center of mass is independent of their spinning. This implies that both motor translational kinetic energy and gravitational potential energy do not depend on q_2, and can, therefore, be modelled by including each motor mass in the respective expressions for each link.

These are the assumptions made by [1], that include also, and are more strict of, the ones made by [2], in which the first assumption is not made.

2.2 Lagrangian Dynamics

Under the assumptions listed above, the model can be derived analytically using the known Lagrangian approach. The kinetic energy T of the system is

$$T = \frac{1}{2}\dot{\mathbf{q}}^\top \mathbf{M}(\mathbf{q}_1)\dot{\mathbf{q}} + \frac{1}{2}\dot{\mathbf{q}}_2^\top \mathbf{J}\dot{\mathbf{q}}_2 = \frac{1}{2}\begin{pmatrix}\dot{\mathbf{q}}_1^\top & \dot{\mathbf{q}}_2^\top\end{pmatrix}\begin{pmatrix}\mathbf{M}(\mathbf{q}_1) & \mathbf{0} \\ \mathbf{0} & \mathbf{J}\end{pmatrix}\begin{pmatrix}\dot{\mathbf{q}}_1 \\ \dot{\mathbf{q}}_2\end{pmatrix} \tag{2.3}$$

where $\mathbf{M}(\mathbf{q}_1)$ is the usual inertia matrix of the "rigid" robot, while $\mathbf{J}$ is the "motor" inertia matrix, defined as $\mathbf{J} \triangleq diag\left\{rg_1^2 I_{zz_1}, \ldots, rg_n^2 I_{zz_n}\right\}$, with $\mathbf{I}_i$ being the inertia tensor of the i-th motor. Notice that by assumption 1, there is no inertial coupling between $\dot{\mathbf{q}}_1, \dot{\mathbf{q}}_2$.
The potential energy of the system is

$$U = U_{el} + U_g = \frac{1}{2}(\mathbf{q}_1 - \mathbf{q}_2)^\top \mathbf{K}(\mathbf{q}_1 - \mathbf{q}_2) + \sum_{i=1}^{n} -m_i \mathbf{g}^\top \mathbf{r}_{0,c_i} \tag{2.4}$$

where $\mathbf{K} = diag\{k_1, \ldots, k_n\}$ is a diagonal matrix holding the elastic constants, m_i is the mass of link (and motor) i, $\mathbf{r}_{0,c_i}$ is the position of the center of mass of link (and motor) i expressed in some "base" frame RF_0.
Following the Lagrangian approach, one defines the Lagrangian of the system as $L \triangleq T - U$ and applying the Euler-Lagrange equations gets

$$\frac{\mathrm{d}}{\mathrm{d}t}\left(\frac{\partial L}{\partial \dot{\mathbf{q}}}\right)^\top - \left(\frac{\partial L}{\partial \mathbf{q}}\right)^\top = \mathbf{u} \tag{2.5}$$

that yields the dynamical model

$$\begin{aligned}\mathbf{M}(\mathbf{q}_1)\ddot{\mathbf{q}}_1 + \mathbf{c}(\mathbf{q}_1, \dot{\mathbf{q}}_1) + \mathbf{g}(\mathbf{q}_1) + \mathbf{K}(\mathbf{q}_1 - \mathbf{q}_2) &= \mathbf{0} \\ \mathbf{J}\ddot{\mathbf{q}}_2 - \mathbf{K}(\mathbf{q}_1 - \mathbf{q}_2) &= \mathbf{u},\end{aligned} \tag{2.6}$$

where as usual it is

$$\mathbf{g}(\mathbf{q}_1) = \frac{\partial U_g}{\partial \mathbf{q}_1}, \quad \mathbf{c}(\mathbf{q}_1, \dot{\mathbf{q}}_1) = \sum_{i=1}^{n}\left(\frac{\partial \mathbf{M}_i}{\partial \mathbf{q}} - \frac{1}{2}\left(\frac{\partial \mathbf{M}_i}{\partial \mathbf{q}}\right)^\top\right)\dot{\mathbf{q}}_i\dot{\mathbf{q}}.$$

The model retains all the structural properties we are familiar with, for instance the Coriolis and centrifugal term $\mathbf{c}(\mathbf{q}_1, \dot{\mathbf{q}}_1)$ being factorizable as $\mathbf{S}(\mathbf{q}_1, \dot{\mathbf{q}}_1)\dot{\mathbf{q}}_1$, with the factorization matrix $\mathbf{S}$ constructed through the Christoffel symbols, leading to $\dot{\mathbf{M}} - 2\mathbf{S}$ being skew-symmetric.

2.3 State space

The dynamical model (2.6) can be expressed in state-space by defining a $4n \times 1$ state vector $\mathbf{x} = \left(\mathbf{x}_1^\top, \mathbf{x}_2^\top, \mathbf{x}_3^\top, \mathbf{x}_4^\top\right)^\top$ with

$$\mathbf{x}_1 = \mathbf{q}_1, \quad \mathbf{x}_2 = \dot{\mathbf{q}}_1, \quad \mathbf{x}_3 = \mathbf{q}_2, \quad \mathbf{x}_4 = \dot{\mathbf{q}}_2 \tag{2.7}$$

as done by [1]. Then, the system has dynamics:

$$\dot{\mathbf{x}}_1 = \mathbf{x}_2 \tag{2.8}$$
$$\dot{\mathbf{x}}_2 = -\mathbf{M}(\mathbf{x}_1)^{-1}\left(\mathbf{c}(\mathbf{x}_1, \mathbf{x}_2) + \mathbf{g}(\mathbf{x}_1) + \mathbf{K}(\mathbf{x}_1 - \mathbf{x}_3)\right) \tag{2.9}$$
$$\dot{\mathbf{x}}_3 = \mathbf{x}_4 \tag{2.10}$$
$$\dot{\mathbf{x}}_4 = \mathbf{J}^{-1}\left(\mathbf{K}(\mathbf{x}_1 - \mathbf{x}_3) + \mathbf{u}\right) \tag{2.11}$$

3 Observers Design

For the estimate of the full state, the optimal solution would be to use, as measurements, motors' positions and velocities since most robots are equipped with sensors on the motor shaft. Unfortunately, observers using such measurements do not exist. Henceforth, links' positions $\mathbf{q}_1$ and, at most, their time rates $\dot{\mathbf{q}}_1$ are assumed to be available for measurement.
On the basis of the dynamical model developed in the previous section, it is possible to derive at least two different observers.

3.1 Observer 1 (Tomei observer)

A first observer, which requires the measurements of both $\mathbf{q}_1$ and $\dot{\mathbf{q}}_1$, is the one proposed by Tomei in [2].
Denoting by $\widehat{\mathbf{q}}$ the estimate of $\mathbf{q}$, the observer has the following structure:

$$\begin{aligned} \mathbf{M}(\mathbf{q}_1)\ddot{\widehat{\mathbf{q}}}_1 + \mathbf{S}(\mathbf{q}_1, \dot{\mathbf{q}}_1)\dot{\widehat{\mathbf{q}}}_1 + \mathbf{K}(\widehat{\mathbf{q}}_1 - \widehat{\mathbf{q}}_2) + \mathbf{g}(\mathbf{q}_1) &= \mathbf{K}_a(\mathbf{q}_1 - \widehat{\mathbf{q}}_1) - \mathbf{v}_1 \\ \mathbf{J}\ddot{\widehat{\mathbf{q}}}_2 - \mathbf{K}(\widehat{\mathbf{q}}_1 - \widehat{\mathbf{q}}_2) &= \mathbf{u} \end{aligned} \tag{3.1}$$

where

- $\mathbf{K}_a$ is an $n \times n$ positive definite matrix,
- $\mathbf{v}_1$ is an $n \times 1$ vector defined as follows.

$$\begin{aligned} \dot{\mathbf{z}} &= -\mathbf{A}\mathbf{z} + (\dot{\mathbf{q}}_1 - \dot{\widehat{\mathbf{q}}}_1) \\ \mathbf{v}_1 &= -\mathbf{K}_1\mathbf{z} - \mathbf{K}_2(\dot{\mathbf{q}}_1 - \dot{\widehat{\mathbf{q}}}_1) \end{aligned} \tag{3.2}$$

where

- $\mathbf{A}$ and $\mathbf{K}_2$ are $n \times n$ positive definite matrices
- $\mathbf{K}_1$ is an $n \times n$ matrix solution of the Lyapunov equation $\mathbf{A}^\top\mathbf{K}_1 + \mathbf{K}_1 A = \mathbf{Q}$ with $\mathbf{Q}$ symmetric and positive definite

Defining the estimation error $\tilde{\mathbf{q}} \triangleq \mathbf{q} - \widehat{\mathbf{q}}$, its dynamics is:

$$\begin{aligned} \mathbf{M}(\mathbf{q}_1)\ddot{\tilde{\mathbf{q}}}_1 + \mathbf{S}(\mathbf{q}_1, \dot{\mathbf{q}}_1)\dot{\tilde{\mathbf{q}}}_1 + \mathbf{K}(\tilde{\mathbf{q}}_1 - \tilde{\mathbf{q}}_2) - \mathbf{K}_a\tilde{\mathbf{q}}_1 &= \mathbf{v}_1 \\ \mathbf{J}\ddot{\tilde{\mathbf{q}}}_2 - \mathbf{K}(\tilde{\mathbf{q}}_1 - \tilde{\mathbf{q}}_2) &= \mathbf{0}. \end{aligned} \tag{3.3}$$

In view of the above equations, the state of the dynamical system associated with the evolution of the error is

$$\mathbf{x}^\top \triangleq \begin{bmatrix} \tilde{\mathbf{q}}^\top & \dot{\tilde{\mathbf{q}}}^\top & \mathbf{z}^\top \end{bmatrix}^\top \tag{3.4}$$

Note that the unique equilibrium point is $\mathbf{x} = \mathbf{0}$. The following result holds true.

Theorem 3.1. *Consider the system described by* (3.2) - (3.4). *If the link velocities* $\dot{\mathbf{q}}_1(t)$ *are bounded, then* $\lim_{t\to\infty} \mathbf{x}(t) = \mathbf{0}$.

Proof. See proof of Theorem 1 in [2]. □

Remark 3.1. From the above theorem it follows, being system (3.2) - (3.4) time varying, that the equilibrium point $x = 0$ is uniformly asymptotically stable.

Remark 3.2. The observer can be modified in order to estimate links' accelerations and jerks, for the details see [2]. This may be very useful since some control laws, like the ones presented in [1], require the knowledge of the aforesaid quantities. It should also be stressed out that it is possible to compute an estimate of the links' accelerations and jerks through an estimate of motors' positions and velocities, like shown in [1].

3.2 Observer 2 (Ciccarella - Germani observer)

A second observer, which requires in principle only the measurement of the links' positions, can be derived extending to the MIMO context the theory developed in [3].
For the sake of brevity, the reader is referred to look at appendix A for the proofs of the following claims.
Consider a nonlinear (square) MIMO system of the form

$$\begin{aligned} \dot{\mathbf{x}} &= \mathbf{f}(\mathbf{x}) + \mathbf{G}(\mathbf{x})\mathbf{u} = \mathbf{f}(\mathbf{x}) + \sum_{i=1}^{m} g_i(\mathbf{x})u_i \\ \mathbf{y} &= \mathbf{H}(\mathbf{x}) = \begin{bmatrix} h_1(\mathbf{x}) \\ \vdots \\ h_m(\mathbf{x}) \end{bmatrix} \end{aligned} \tag{3.5}$$

where $\mathbf{x} \in \mathbb{R}^n$ is the state of the system, $\mathbf{u} \in \mathbb{R}^m$ is the input to the system and $\mathbf{y} \in \mathbb{R}^m$ is the output of the system.
The following claim extends Theorem 2 in [3].

Claim 3.1. *Suppose system* (3.5) *has vector relative degree* $\mathbf{r} = \begin{bmatrix} r_1, \ldots, r_m \end{bmatrix}^\top$ *such that* $r_1 + \cdots + r_m = n$. *Let* $\mathbf{U}(\mathbf{x})$ *be the* decoupling matrix *[4] of the system:*

$$\mathbf{U}(\mathbf{x}) = \begin{bmatrix} L_{g_1}L_f^{r_1-1}h_1 & \ldots & L_{g_m}L_f^{r_1-1}h_1 \\ \vdots & \ddots & \vdots \\ L_{g_1}L_f^{r_m-1}h_m & \ldots & L_{g_m}L_f^{r_m-1}h_m \end{bmatrix}, \tag{3.6}$$

and let $\mathbf{Q}(\mathbf{x})$ *be defined as*

$$\mathbf{Q}(\mathbf{x}) \triangleq \frac{\mathrm{d}}{\mathrm{d}\mathbf{x}} \begin{bmatrix} h_1 \\ \vdots \\ L_f^{r_1-1} h_1 \\ \hline h_2 \\ \vdots \\ L_f^{r_2-1} h_2 \\ \hline \vdots \\ \hline h_m \\ \vdots \\ L_f^{r_m-1} h_m \end{bmatrix}. \tag{3.7}$$

If

(H1) $rank(\mathbf{Q}(\mathbf{x})) = n$.

(H2) The vector

$$\begin{bmatrix} L_f^{r_1} h_1(\mathbf{\Phi}^{-1}(\mathbf{z})) \\ \vdots \\ L_f^{r_m} h_m(\mathbf{\Phi}^{-1}(\mathbf{z})) \end{bmatrix} + \mathbf{U}(\Phi^{-1}(\mathbf{z}))\mathbf{u} \tag{3.8}$$

is uniformly Hölder for all bounded inputs $\mathbf{u}$*, i.e.*

$$\begin{gathered} \forall \boldsymbol{\zeta}_1, \boldsymbol{\zeta}_2 \in \mathbb{R}^n \quad \exists \gamma > 0, \delta \in (0,1] \quad \textit{such that} \\ \sup_{\|\mathbf{u}\| \leq M} \left\| \left(\begin{bmatrix} L_f^{r_1} h_1(\mathbf{\Phi}^{-1}(\boldsymbol{\zeta}_1)) \\ \vdots \\ L_f^{r_m} h_m(\mathbf{\Phi}^{-1}(\boldsymbol{\zeta}_1)) \end{bmatrix} + \mathbf{U}(\mathbf{\Phi}^{-1}(\boldsymbol{\zeta}_1))\mathbf{u} \right) - \left(\begin{bmatrix} L_f^{r_1} h_1(\mathbf{\Phi}^{-1}(\boldsymbol{\zeta}_2)) \\ \vdots \\ L_f^{r_m} h_m(\mathbf{\Phi}^{-1}(\boldsymbol{\zeta}_2)) \end{bmatrix} + \mathbf{U}(\mathbf{\Phi}^{-1}(\boldsymbol{\zeta}_2))\mathbf{u} \right) \right\| \\ \leq \gamma \|\boldsymbol{\zeta}_1 - \boldsymbol{\zeta}_2\|^{\delta} \end{gathered} \tag{3.9}$$

then there exists a collection of finite gain vectors $\mathbf{K}_1 \in \mathbb{R}^{r_1}, \ldots, \mathbf{K}_m \in \mathbb{R}^{r_m}$ *such that the following system of equations*

$$\dot{\hat{\mathbf{x}}} = \mathbf{f}(\hat{\mathbf{x}}) + \mathbf{G}(\hat{\mathbf{x}})\mathbf{u} + \mathbf{Q}(\hat{\mathbf{x}})^{-1} \begin{bmatrix} \mathbf{K}_1 & 0 & \ldots & 0 \\ 0 & \mathbf{K}_2 & \ldots & 0 \\ \vdots & \vdots & \ddots & 0 \\ 0 & 0 & \ldots & \mathbf{K}_m \end{bmatrix} (\mathbf{y} - \mathbf{H}(\hat{\mathbf{x}})) \tag{3.10}$$

has the following properties:

1. *When* $\delta \in (0,1)$*, for any* $\epsilon > 0, \hat{\mathbf{x}}(0) \in \mathbb{R}^n$ *we have*

$$\lim_{t \to \infty} \|\hat{\mathbf{x}}(t) - \mathbf{x}(t)\| \leq \epsilon. \tag{3.11}$$

2. *When* $\delta = 1$*, for any* $\hat{\mathbf{x}}(0) \in \mathbb{R}^n$ *we have*

$$\lim_{t \to \infty} \|\hat{\mathbf{x}}(t) - \mathbf{x}(t)\| = 0. \tag{3.12}$$

Proof. See proof of theorem A.2. □

Corollary 3.1. *The estimation error for the observer* (3.10) *converges exponentially to zero if*

(i) $\begin{bmatrix} L_f^{r_1} h_1(\mathbf{\Phi}^{-1}(\mathbf{z})) \\ \vdots \\ L_f^{r_m} h_m(\mathbf{\Phi}^{-1}(\mathbf{z})) \end{bmatrix}$ *and* $U(\Phi^{-1}(z))$ *are locally Lipschitz;*

(ii) there exists a closed bounded sphere $S(\rho)$ *of radius* ρ *such that* $\mathbf{x}(t) \in S(\rho), \forall \mathbf{u} \in U$

(iii) $\mathbf{Q}(\mathbf{x})$ *has full rank for all* $\mathbf{x} \in S(radius\{(\mathbf{\Phi}^{-1}(S(Nr+r))\})$ *where* $N > 1$ *is an arbitrarily fixed constant and* r *is such that* $\|\mathbf{\Phi}(\mathbf{x})\| \leq r$ *for all* $\mathbf{x} \in S(\rho)$

(iv) $\|\hat{\mathbf{x}}(0) - \mathbf{x}(0)\| \leq \Psi$ *for a suitable* $\Psi > 0$

Proof. See proof of corollary A.1. □

The above corollary can be applied for estimating the state of a robot with elastic joints using only the links' positions as measurements.
Consider the system in the state space representation (2.8) - (2.11) and, as output $\mathbf{y}$, the links' positions, i.e.

$$\mathbf{y} \triangleq \mathbf{x}_1 = \mathbf{q}_1 \in \mathbb{R}^n, \tag{3.13}$$

then:

Claim 3.2. *The vector relative degree for system (2.8) - (2.11) with output* (3.13) *is*

$$\mathbf{r} = \begin{bmatrix} r_1 & r_2 & \cdots & r_n \end{bmatrix}^\top = \begin{bmatrix} 4 & 4 & \cdots & 4 \end{bmatrix}^\top \tag{3.14}$$

Thus $r_1 + r_2 + \cdots + r_n = 4n$.

Proof. See proof of claim A.1. □

Claim 3.3. *Let* $\mathbf{Q}(\mathbf{x})$ *be the matrix defined accordingly to* (3.7) *for system (2.8) - (2.11) with output* (3.13)*, i.e.*

$$\mathbf{Q}(\mathbf{x}) = \frac{\mathrm{d}}{\mathrm{d}\mathbf{x}} \left[\begin{array}{c} x_1^{(1)} \\ L_f x_1^{(1)} \\ L_f^2 x_1^{(1)} \\ L_f^3 x_1^{(1)} \\ \hline \vdots \\ \hline x_1^{(n)} \\ L_f x_1^{(n)} \\ L_f^2 x_1^{(n)} \\ L_f^3 x_1^{(n)} \end{array}\right], \tag{3.15}$$

where $x_1^{(i)}$ *denotes the* i*-th component of* $\mathbf{x}_1 = \mathbf{q}_1$*. Then,* $\mathbf{Q}(\mathbf{x})$ *is nonsingular for any* $\mathbf{x}$.

Proof. See proof of claim A.2. □

Claim 3.4. *The vector*

$$L_f^4\mathbf{H}\Big|_{\mathbf{x}=\mathbf{\Phi}^{-1}(\mathbf{z})} = \begin{bmatrix} L_f^4 x_1^{(1)} \\ \vdots \\ L_f^4 x_1^{(n)} \end{bmatrix}\Bigg|_{\mathbf{x}=\mathbf{\Phi}^{-1}(\mathbf{z})} \tag{3.16}$$

is locally Lipschitz.

Proof. See proof of claim A.3. □

Claim 3.5. *The matrix*

$$\mathbf{U}(\mathbf{x})\Big|_{\mathbf{x}=\mathbf{\Phi}^{-1}(\mathbf{z})} \tag{3.17}$$

where $\mathbf{U}(\mathbf{x})$ *denotes the decoupling matrix of system (2.8) - (2.11) with output* (3.13) *is a locally Lipschitz map.*

Proof. See proof of claim A.4. □

Thanks to the above claims, one can use an observer of the form (3.10) to estimate the state of the robot using only the measurements of the links' positions. In this sense this observer is better than the previous one because it requires, in principle, less measurements to reconstruct the whole state. In addition, many times is not possible to measure directly the links' velocites and, using numerical differentiation algorithms, only estimates can be produced.

Remark 3.3. If one assumes to have also a measure of the links' velocities, with some modifications, it is possible to arrive at conclusions similar to the one above, i.e. one can implement an observer for (2.8) - (2.11) which corrects the estimate using also the estimation error on the links' velocities. In this scenario such observer is expected to perform better, or at least, to be more robust than the one which uses only links' positions, a fact that we have experienced in simulations.

Thanks to the following two claims other two observers can be implemented. A first one uses, as output, the motors' positions and the elastic torque. A second one which uses the motors' positions and the links' accelerations.

Claim 3.6. *The vector relative degree for the system (2.8) - (2.11) with output*

$$\mathbf{y} \triangleq \begin{bmatrix} \mathbf{x}_3^\top & (K(\mathbf{x}_1 - \mathbf{x}_3))^\top \end{bmatrix}^\top,$$

with, $\mathbf{y} \in \mathbb{R}^{2n}$*, is:*

$$\mathbf{r} = \begin{bmatrix} r_1 & r_2 & \cdots & r_n & r_{n+1} & \cdots & r_{2n} \end{bmatrix}^\top = \begin{bmatrix} 2 & 2 & \cdots & 2 & 2 & \cdots & 2 \end{bmatrix}^\top \tag{3.18}$$

Thus $r_1 + r_2 + \cdots + r_n + r_{n+1} + \cdots + r_{2n} = 4n$*.*

Proof. See proof of claim A.5. □

Claim 3.7. *The vector relative degree for the system (2.8) - (2.11) with output*

$$\mathbf{y} \triangleq \begin{bmatrix} \mathbf{x}_3^\top & \ddot{\mathbf{x}}_1^\top \end{bmatrix}^\top,$$

with $\mathbf{y} \in \mathbb{R}^{2n}$*, is:*

$$\mathbf{r} = \begin{bmatrix} r_1 & r_2 & \cdots & r_n & r_{n+1} & \cdots & r_{2n} \end{bmatrix}^\top = \begin{bmatrix} 2 & 2 & \cdots & 2 & 2 & \cdots & 2 \end{bmatrix}^\top \tag{3.19}$$

Thus $r_1 + r_2 + \cdots + r_n + r_{n+1} + \cdots + r_{2n} = 4n$*.*

Proof. See proof of claim A.6. □

4 Controllers Design

In this section, we summarize the Feedback Linearizing controller and Integral Manifold controller developed in [1] to which the reader is referred to look at for all the details.

4.1 Feedback Linearizing Controller

This controller allows to linearize the system dynamics and to obtain a controllable, LTI and decoupled system (in which every I/O channel appears as a chain of four integrators) in a new set of coordinates. The control scheme is composed of two parts since the control input $\mathbf{u}$, in turn, contains a new control input $\boldsymbol{\nu}$ acting on the linearized dynamics.
Consider the nonlinear state space change of coordinates $\mathbf{y} = \mathbf{T}(\mathbf{x})$ (see [1] for all the details) applied to the system (2.8) - (2.11):

$$\mathbf{y}_1 = \mathbf{T}_1(\mathbf{x}) = \mathbf{x}_1 \tag{4.1}$$

$$\mathbf{y}_2 = \mathbf{T}_2(\mathbf{x}) = \dot{\mathbf{T}}_1 = \mathbf{x}_2 \tag{4.2}$$

$$\mathbf{y}_3 = \mathbf{T}_3(\mathbf{x}) = \dot{\mathbf{T}}_2 = -\mathbf{M}(\mathbf{x}_1)^{-1}\left(\mathbf{c}(\mathbf{x}_1, \mathbf{x}_2) + \mathbf{g}(\mathbf{x}_1) + \mathbf{K}(\mathbf{x}_1 - \mathbf{x}_3)\right) \tag{4.3}$$

$$\mathbf{y}_4 = \mathbf{T}_4(\mathbf{x}) = \dot{\mathbf{T}}_3 = \cdots = \mathbf{f}_4(\mathbf{x}_1, \mathbf{x}_2, \mathbf{x}_3) + \mathbf{M}(\mathbf{x}_1)^{-1}\mathbf{K}\mathbf{x}_4. \tag{4.4}$$

Notice that the new set of variables $\mathbf{y}_1, \ldots, \mathbf{y}_4$ are physically meaningful, since they represent, respectively, the link positions, velocities, accelerations, and jerks.
In order to obtain $\dot{\mathbf{y}}_4 = \boldsymbol{\nu}$, with $\boldsymbol{\nu}$ a new control input, one sets:

$$\mathbf{u} = \mathbf{J}\mathbf{K}^{-1}\mathbf{M}(\mathbf{x}_1)\left(\boldsymbol{\nu} - \mathbf{F}(\mathbf{x})\right) \tag{4.5}$$

where $\mathbf{F}(\mathbf{x})$ collects all the terms that do not contain $\mathbf{u}$ in the expansion of $\dot{y}_4$, for the sake of clarity.
By definition of $\mathbf{y}$ and $\boldsymbol{\nu}$ the system (2.8) - (2.11), in the new coordinates, has the following block linear dynamics:

$$\dot{\mathbf{y}} = \mathbf{A}\mathbf{y} + \mathbf{B}\boldsymbol{\nu} = \begin{bmatrix} \mathbf{0} & \mathbf{I} & \mathbf{0} & \mathbf{0} \\ \mathbf{0} & \mathbf{0} & \mathbf{I} & \mathbf{0} \\ \mathbf{0} & \mathbf{0} & \mathbf{0} & \mathbf{I} \\ \mathbf{0} & \mathbf{0} & \mathbf{0} & \mathbf{0} \end{bmatrix} \mathbf{y} + \begin{bmatrix} \mathbf{0} \\ \mathbf{0} \\ \mathbf{0} \\ \mathbf{I} \end{bmatrix} \boldsymbol{\nu}. \tag{4.6}$$

Clearly, the nonlinear control law (4.5) is not completely determined until the function $\boldsymbol{\nu}$ is specified. For instance, [1] shows that it is possible to design $\boldsymbol{\nu}$ so as to guarantee robust tracking for the above systems. In fact, suppose to have a desired differentiable trajectory[1] $\mathbf{y}^d$; by setting

$$\boldsymbol{\nu} = \dot{\mathbf{y}}_4^d + \mathbf{K}_P\mathbf{e} + \boldsymbol{\Delta\nu} \tag{4.7}$$

where $\mathbf{e}$ is the tracking error $\mathbf{e} \triangleq \mathbf{y} - \mathbf{y}^d$, $\mathbf{K}_P$ is a gain matrix such that $\mathbf{A} + \mathbf{B}\mathbf{K}_P$ is stable, and $\boldsymbol{\Delta\nu}$ is a new control input, one has tracking error dynamics

$$\dot{\mathbf{e}} = \mathbf{A}\mathbf{e} + \mathbf{B}\left(\boldsymbol{\Delta\nu} + \boldsymbol{\Psi}\right) \tag{4.8}$$

where $\boldsymbol{\Psi}$ is an "uncertainty" term. Spong in [1] has shown this dynamics to be uniformly asymptotically stabilized to zero by a suitable choice of $\boldsymbol{\Delta\nu}$ by exploiting certain assumptions on the boundedness of the parameter estimation error.

[1] Note that actually $\mathbf{y}$, by definition, represents joints position and their derivatives up to the third order.

4.2 Integral Manifold Controller

This controller is obtained starting from a reformulation of the dynamic equations (2.6) as a singularly perturbed system. With reference to (2.6), set

$$\begin{aligned} \mathbf{z} &\triangleq \mathbf{K}(\mathbf{q}_1 - \mathbf{q}_2) \\ \boldsymbol{\mu} &\triangleq \mathbf{K}^{-1} \end{aligned} \tag{4.9}$$

The vector $\mathbf{z}$ is the elastic force at the joints. In the coordinates coordinates $\mathbf{q}_1$ and $\mathbf{z}$, the robot dynamics is:

$$\begin{aligned} \ddot{\mathbf{q}}_1 &= -\mathbf{M}(\mathbf{q}_1)^{-1}\left(\mathbf{c}(\mathbf{q}_1, \dot{\mathbf{q}}_1) + \mathbf{g}(\mathbf{q}_1)\right) - \mathbf{M}(\mathbf{q}_1)^{-1}\mathbf{z} \\ &\triangleq \mathbf{a}_1(\mathbf{q}, \dot{\mathbf{q}}) + \mathbf{A}_1(\mathbf{q})\mathbf{z} \\ \boldsymbol{\mu}\ddot{\mathbf{z}} &= -\mathbf{M}(\mathbf{q}_1)^{-1}\left(\mathbf{c}(\mathbf{q}_1, \dot{\mathbf{q}}_1) + \mathbf{g}(\mathbf{q}_1)\right) - (\mathbf{M}(\mathbf{q}_1)^{-1} + \mathbf{J}^{-1})\mathbf{z} - \mathbf{J}^{-1}\mathbf{u} \\ &\triangleq \mathbf{a}_2(\mathbf{q}, \dot{\mathbf{q}}) + \mathbf{A}_2(\mathbf{q})\mathbf{z} + \mathbf{B}_2\mathbf{u} \end{aligned} \tag{4.10}$$

where the subscript on $\mathbf{q}$ has been removed for convenience. The above model is singularly perturbed; indeed, notice that as $\boldsymbol{\mu}$ goes to $\mathbf{0}$, (4.10) reduces to the rigid equations of motion. In the $4n$-dimensional state space defined by (4.9), is considered a $2n$-dimensional manifold $M_{\boldsymbol{\mu}}$ defined through the equations

$$\begin{aligned} \mathbf{z} &= \mathbf{h}(\mathbf{q}, \dot{\mathbf{q}}, \mathbf{u}, \boldsymbol{\mu}) \\ \dot{\mathbf{z}} &= \dot{\mathbf{h}}(\mathbf{q}, \dot{\mathbf{q}}, \mathbf{u}, \boldsymbol{\mu}) \end{aligned} \tag{4.11}$$

Definition 1. *The manifold $M_{\boldsymbol{\mu}}$ is said to be an integral manifold for* (4.11) *if it is invariant under solutions of the system, i.e. given an admissible input $\mathbf{u}(t)$, if the initial state*

$$\begin{bmatrix} \mathbf{q}_1(t_0) & \dot{\mathbf{q}}_1(t_0) & \mathbf{z}(t_0) & \dot{\mathbf{z}}(t_0) \end{bmatrix}^\top$$

of system (4.11) *lies on $M_{\boldsymbol{\mu}}$, that is*

$$\begin{aligned} \mathbf{z}(t_0) &= \mathbf{h}(\mathbf{q}_1(t_0), \dot{\mathbf{q}}_1(t_0), \mathbf{u}(t_0), \boldsymbol{\mu}) \\ \dot{\mathbf{z}}(t_0) &= \dot{\mathbf{h}}(\mathbf{q}_1(t_0), \dot{\mathbf{q}}_1(t_0), \mathbf{u}(t_0), \boldsymbol{\mu}), \end{aligned} \tag{4.12}$$

then the state of the system

$$\begin{bmatrix} \mathbf{q}_1(t) & \dot{\mathbf{q}}_1(t) & \mathbf{z}(t) & \dot{\mathbf{z}}(t) \end{bmatrix}^\top$$

remains in $M_{\boldsymbol{\mu}}$ for all $t > t_0$, that is

$$\begin{aligned} \mathbf{z}(t) &= \mathbf{h}(\mathbf{q}_1(t), \dot{\mathbf{q}}_1(t), \mathbf{u}(t), \boldsymbol{\mu}) \quad \forall t > t_0 \\ \dot{\mathbf{z}}(t) &= \dot{\mathbf{h}}(\mathbf{q}_1(t), \dot{\mathbf{q}}_1(t), \mathbf{u}(t), \boldsymbol{\mu}) \quad \forall t > t_0 \end{aligned} \tag{4.13}$$

To compute analytically the equations of the integral manifold, in view of the second term in (4.10) and of (4.11), one has to find a function $\mathbf{h}$, not unique, which solves the following P.D.E.

$$\boldsymbol{\mu}\ddot{\mathbf{h}} = \mathbf{a}_2(\mathbf{q}, \dot{\mathbf{q}}) + \mathbf{A}_2(\mathbf{q})\mathbf{h} + \mathbf{B}_2\mathbf{u} \tag{4.14}$$

The input $\mathbf{u}$ is set to

$$\mathbf{u} \triangleq \mathbf{u}_s(\mathbf{q}, \dot{\mathbf{q}}, \boldsymbol{\nu}, \boldsymbol{\mu}) + \mathbf{u}_f(\boldsymbol{\eta}, \dot{\boldsymbol{\eta}}), \tag{4.15}$$

with $\mathbf{u}_f(\mathbf{0}, \mathbf{0}) = \mathbf{0}$ so that $\mathbf{u} = \mathbf{u}_s$ on $M_{\boldsymbol{\mu}}$, where

- vector $\boldsymbol{\nu}$ represents an extra command to be specified
- vector $\boldsymbol{\eta}$ represents the devation of the *fast variables* $\mathbf{z}$ from the integral manifold, i.e.

$$\begin{aligned} \boldsymbol{\eta} &\triangleq \mathbf{z} - \mathbf{h}(\mathbf{q}, \dot{\mathbf{q}}, \mathbf{u}_s, \boldsymbol{\mu}) \\ \dot{\eta} &\triangleq \dot{\mathbf{z}} - \dot{\mathbf{h}}(\mathbf{q}, \dot{\mathbf{q}}, \mathbf{u}_s, \boldsymbol{\mu}) \end{aligned} \tag{4.16}$$

Expanding $\mathbf{h}$ in power series, as a function of $\boldsymbol{\mu}$, and setting

$$\mathbf{u}_s = \mathbf{u}_0 + \boldsymbol{\mu}\mathbf{u}_1, \tag{4.17}$$

where $\mathbf{u}_0$ and $\mathbf{u}_1$ are specified below, [1] has shown that is possible to enstablish the following identity:

$$\mathbf{h} = -\mathbf{A}_2^{-1}(\mathbf{a}_2 + \mathbf{B}_2\mathbf{u}_0), \tag{4.18}$$

where $\mathbf{u}_0$ can be seen as an extra control input, to be specified later. Given $\mathbf{h}$, computed from (4.18), it is possible to compute $\ddot{\mathbf{h}}$ and, in order to guarantee (4.18) [1], one has to set $\mathbf{u}_1$ as

$$\mathbf{u}_1 = \mathbf{B}_2^{-1}\ddot{\mathbf{h}}. \tag{4.19}$$

The dynamics on $M_{\boldsymbol{\mu}}$ is given by

$$\begin{aligned} \ddot{\mathbf{q}} &= \mathbf{a}_1 - \mathbf{A}_1\mathbf{A}_2^{-1}\mathbf{a}_2 - \mathbf{A}_1\mathbf{A}_2^{-1}\mathbf{B}_2\mathbf{u}_0 \\ &= -(\mathbf{M}(\mathbf{q}_1) + \mathbf{J})^{-1}(\mathbf{c}(\mathbf{q}_1, \dot{\mathbf{q}}_1) + \mathbf{g}(\mathbf{q}_1) + \mathbf{u}_0). \end{aligned} \tag{4.20}$$

Equation (4.20) establishes that on $M_{\boldsymbol{\mu}}$ the robot behaves as if it were rigid and $\mathbf{u}_0$, which can be easily interpreted as the control applied on $M_{\boldsymbol{\mu}}$, is any desired action built on the rigid system. Choosing $\mathbf{u}_0$ so as to linearize the dynamics on the integral manifold, in terms of the state variables $\mathbf{q}$ and $\boldsymbol{\eta}$, the dynamics becomes:

$$\ddot{\mathbf{q}} = \boldsymbol{\nu} + \mathbf{A}_1(\mathbf{q})\boldsymbol{\eta} \tag{4.21}$$

$$\boldsymbol{\mu}\ddot{\boldsymbol{\eta}} = \mathbf{A}_2(\mathbf{q})\boldsymbol{\eta} + \mathbf{B}_2\mathbf{u}_f. \tag{4.22}$$

The *fast control* $\mathbf{u}_f$ is still a design parameter. Since $\mathbf{B}_2$ is non singular, the linear time varying system described by (4.22) is controllable which implies that its poles can be assigned arbitrarly. Depending on the structure of the manipulator, the system may have a natural damping, i.e. $\mathbf{A}_2(\mathbf{q})$ may be such that (4.22), for any possible configuration $\mathbf{q}$, has the origin as a uniformly asymptotically stable equilibrium. In this case $\mathbf{u}_f$ can be set to $\mathbf{0}$.
Otherwise one can set

$$\mathbf{u}_f = \mathbf{B}_2^{-1}(\boldsymbol{\zeta} - \mathbf{A}_2(\mathbf{q})\boldsymbol{\eta}) \tag{4.23}$$

so that the following linear, controllable and decoupled system is obtained:

$$\begin{aligned} \ddot{\mathbf{q}} &= \boldsymbol{\nu} + \mathbf{A}_1(\mathbf{q})\boldsymbol{\eta} \\ \boldsymbol{\mu}\ddot{\boldsymbol{\eta}} &= \boldsymbol{\zeta} \end{aligned} \tag{4.24}$$

On the above system, through $\boldsymbol{\nu}$ and $\boldsymbol{\zeta}$, any control law can be chosen to obtain a desired behaviour.
In few words the integral manifold developed by Spong is made by two different terms:

- $\mathbf{u}_f$ (*fast* control) is meant to drive the state of the system on $M_{\boldsymbol{\mu}}$;
- $\mathbf{u}_s$ (*slow* control) constrains the state on $M_{\boldsymbol{\mu}}$ and makes the elastic robot, when its state is on $M_{\boldsymbol{\mu}}$, to act like as rigid.

With respect to the feedback linearizing controller, this one has the advantage that it is possible to use directly any control law derived for rigid manipulators.

5 Simulations

In the following, we show the results of the simulations we performed, first on the model of a 2R planar manipulator under gravity, and then on the model of a 3R spatial robot, whose dynamic parameters are reported in table 1 and table 2 respectively. The required task is trajectory tracking: in particular, we command a smooth rest-to-rest trajectory interpolated by a cubic spline, from the downward position to the upward position in half the simulation time ($10s$), therefore performing a "swing up" (see fig. 2). We assume the joints to be able to provide a maximum torque of $200Nm$, therefore the control action is saturated.

	Link 1, 2	Motor 1, 2	
Mass	1	3	$[kg]$
Inertia (all equal)	0.4	0.015	$[kg \cdot m^2]$
Length	0.4	–	$[m]$
CoM distance	0.3	–	$[m]$
Reduction gear	–	50	
Elastic constants	20000		$[N \cdot m^{-1}]$

Table 1: Table of the dynamic parameters of the 3R used in the simulations.

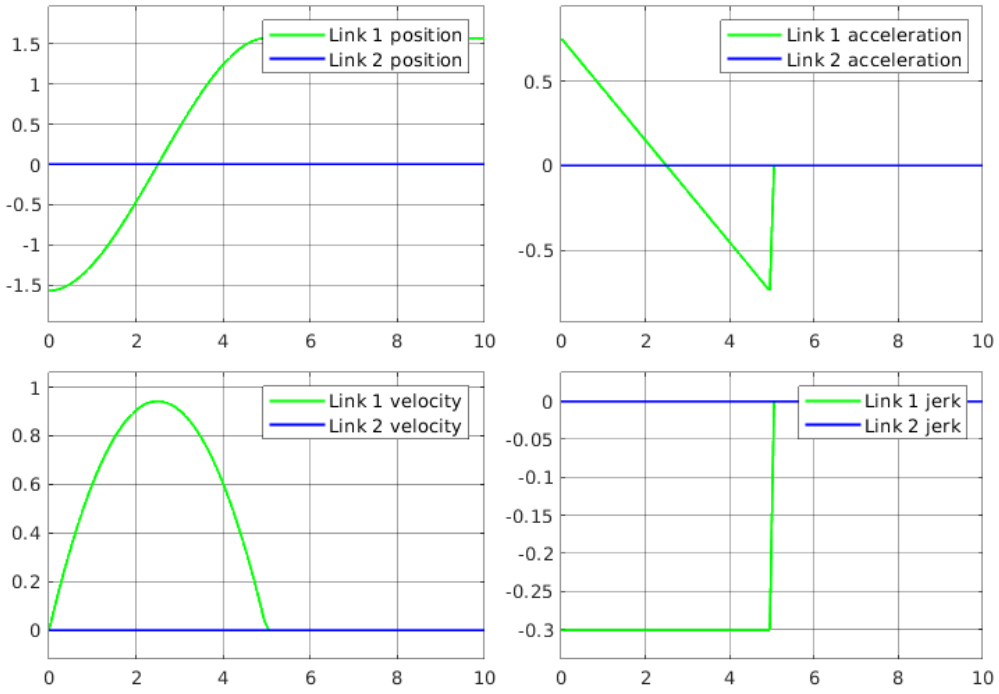

Figure 2: Plot of the desired trajectory for the 2R case.

Simulation 1: Comparison of the observers In the first simulation we compare the behavior of the Tomei and Ciccarella-Germani observers in the 2R case, both inizialized in the same,

partially wrong, estimate of the state: the links position estimates are correctly initialized, while the motor positions are not. More specifically we have:

$$\mathbf{x}_0 = \begin{bmatrix}\mathbf{q}_1(0)^\top & \dot{\mathbf{q}}_1(0)^\top & \mathbf{q}_2(0)^\top & \dot{\mathbf{q}}_2(0)^\top\end{bmatrix}^\top = \begin{bmatrix}-\pi/2, 0 & 0, 0 & -\pi/2, 0 & 0, 0\end{bmatrix}^\top$$
$$\hat{\mathbf{x}}_0 = \begin{bmatrix}\hat{\mathbf{q}}_1(0)^\top & \dot{\hat{\mathbf{q}}}_1(0)^\top & \hat{\mathbf{q}}_2(0)^\top & \dot{\hat{\mathbf{q}}}_2(0)^\top\end{bmatrix}^\top = \begin{bmatrix}-\pi/2, 0 & 0, 0 & 0, 0 & 0, 0\end{bmatrix}^\top$$

The design parameters for the Tomei observer are set as follows:

$$\begin{aligned}\mathbf{A} &= 2000 \cdot \mathbf{I}_n,\\ \mathbf{K}_2 &= 2000 \cdot \mathbf{I}_n,\\ \mathbf{K}_a &= -10000 \cdot \mathbf{I}_n,\end{aligned}$$

while the parameters for the Ciccarella-Germani observer are set as follows:

$$\mathbf{K} \quad \text{such that} \quad \sigma\left(\mathbf{A} - \mathbf{K}\mathbf{C}\right) = -100 \cdot \{3, 4, \ldots, 10\}.$$

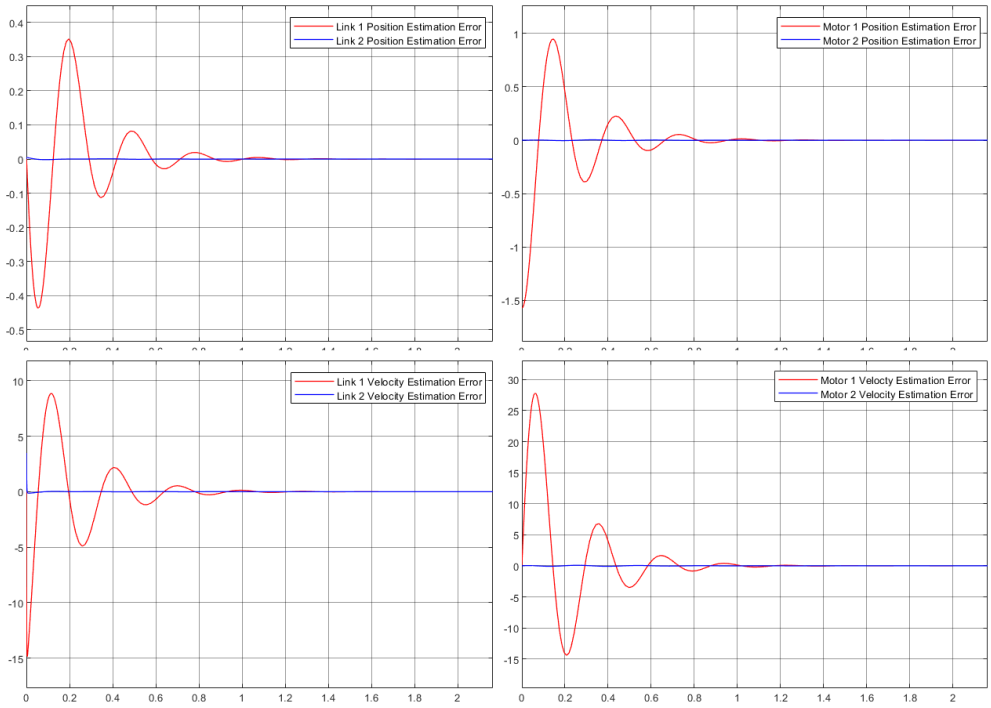

Figure 3: *Simulation 1.* Plot of the estimation error by the Tomei observer.
The Tomei observer is able to drive the estimation error to zero, and thus reconstruct the full state, in approximately 1.4 seconds.

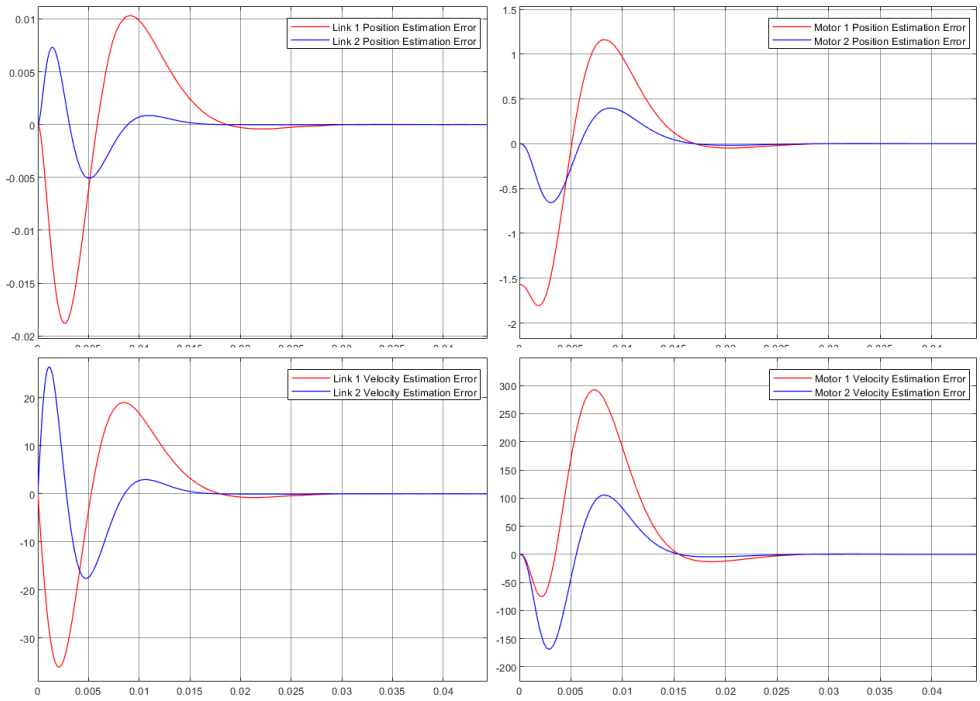

Figure 4: *Simulation 1.* Plot of the estimation error by the Ciccarella-Germani observer. The Ciccarella-Germani observer is able to drive the estimation error to zero, and thus reconstruct the full state, in approximately 0.03 seconds.

It is evident that the Ciccarella-Germani observer exhibits a much faster transient, because of the fast dynamics assigned, although presenting also a significantly more pronounced overshoot on motors velocity estimate. Smaller eigenvalues could be chosen, as long as the conditions of *Remark 4* of [3] are satisfied.
Furthermore, recall from our discussion in section 3 that the Ciccarella-Germani observer only needs the output of the system, assumed to be just the measurement of the position of the links, while the Tomei observer needs measurements of both links positions and velocities. Therefore, it is clear that the Ciccarella-Germani observer definitely outperforms the Tomei observer, with much faster convergence at the "cost" of fewer measurements.
However, we must report also that we have experienced several numerical issues concerning the Ciccarella-Germani observer. In fact, when starting from an initial estimate for the links that is too far off of the actual measurement, the observer becomes unstable, as we will further elaborate below.
We remark however that this instability is not present when the observer is initialized in a state whose links position estimate is "close enough" to the manipulator actual links positions. Finally, notice that we can justify the initialization of the observer in such a state by the assumption of having the position of the links always available for measurement.

Simulation 2: Comparison of the controllers In this simulation we compare the results of simulating the system driven by both controllers, again in the 2R case, both with state feedback and with reconstructed state feedback, to draft a comparison. We have chosen the Ciccarella-Germani observer for this comparison since, as we have demonstrated above, it clearly

outperforms the Tomei observer.
The design parameters for the Feedback Linearizing controller are set as follows:

$$\mathbf{K} \quad \text{such that} \quad \sigma(\mathbf{A}+\mathbf{BK}) = -5 \cdot \{1, 2, \ldots, 8\},$$

while the design parameters for the Integral Manifold controller are set as follows:

$$\begin{aligned} &\mathbf{K}_P = 7000 \cdot \mathbf{I}_n, \\ &\mathbf{K}_D = 7000 \cdot \mathbf{I}_n, \\ &\mathbf{K} \quad \text{such that } \sigma(\mathbf{A}+\mathbf{BK}) = -70 \cdot \{1.1, 1.2, 1.3, 1.4\}. \end{aligned}$$

Notice that we have specified only four controlled dynamics since the controller aims to constrain the manipulator state onto the integral manifold, where it exhibits rigid behavior.

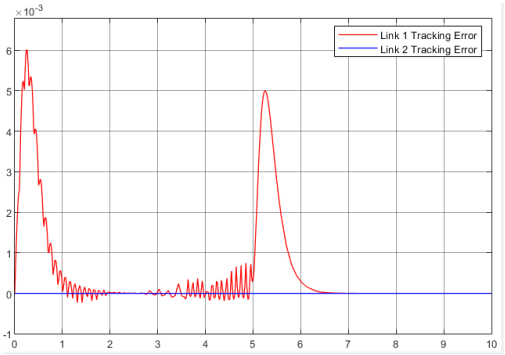

(a) Feedback linearizing controller

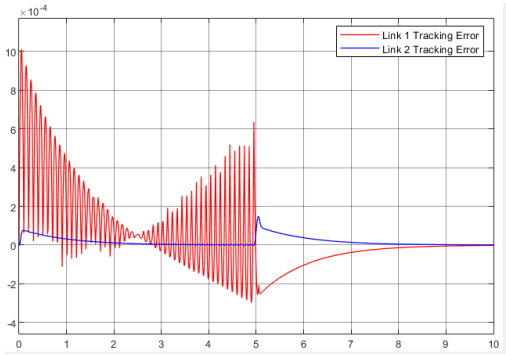

(b) Integral Manifold controller

Figure 5: *Simulation 2.* Plot of the tracking error obtained by the controllers with state feedback.

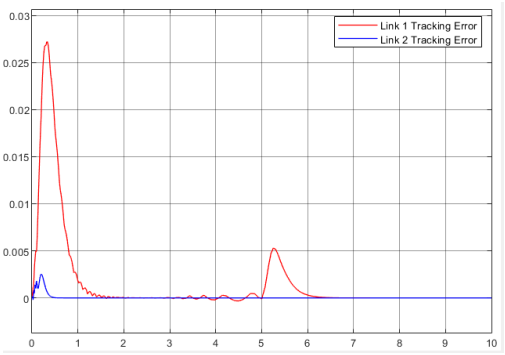

(a) Feedback linearizing controller

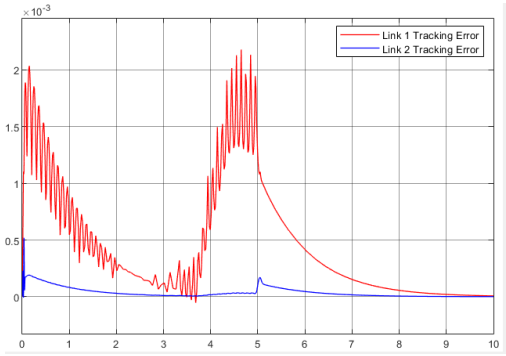

(b) Integral Manifold controller

Figure 6: *Simulation 2.* Tracking error obtained by the controllers with feedback of the state reconstructed by the Ciccarella-Germani observer.

In both scenarios we can see how the Integral Manifold controller outperforms the simpler Feedback Linearizing controller, being able to more accurately track the desired trajectory. The difference in performance is significant when using the reconstructed state as feedback.

Deeper analysis of the Ciccarella-Germani observers In this paragraph, we report various simulations performed to study in more depth the observer by Ciccarella-Germani derived in section 3.2 and to compare the performances of its two versions: the one that uses only the links' positions and the one that employs, as additional measurements, also their time derivatives. We will denote with $\mathcal{O}_1$ and $\mathcal{O}_2$ respectively the observer that uses only the links' positions and the one that uses also the velocities. The simulations we report in this paragraph are performed on a 3R spatial robot with the following dynamic parameters.

	Link 1, 2, 3	Motor 1, 2, 3	
Mass	1	3	$[kg]$
Inertia (all equal)	0.4	0.035	$[kg \cdot m^2]$
Length	0.4	–	$[m]$
CoM distance	0.3	–	$[m]$
Reduction gear	–	50	
Elastic constants	20000		$[N \cdot m^{-1}]$

Table 2: Table of the dynamic parameters of the 3R used in the simulations.

All the considerations done in the next for this 3R robot have been experienced in the same way on the 2R robot. Simulations are perfomed using the manifold controller with the real state of the robot. The first scenario considered is a rest to rest maneuver from the initial position

$$\begin{bmatrix}\mathbf{q}_1^\top & \mathbf{q}_2^\top\end{bmatrix} = \begin{bmatrix}0, \frac{\pi}{2}, 0 & 0, \frac{\pi}{2}, 0\end{bmatrix} \tag{5.1}$$

to the final

$$\begin{bmatrix}\mathbf{q}_1^\top & \mathbf{q}_2^\top\end{bmatrix} = \begin{bmatrix}\frac{\pi}{2}, \pi, 0 & \frac{\pi}{2}, \pi, 0\end{bmatrix}, \tag{5.2}$$

see fig. 7.

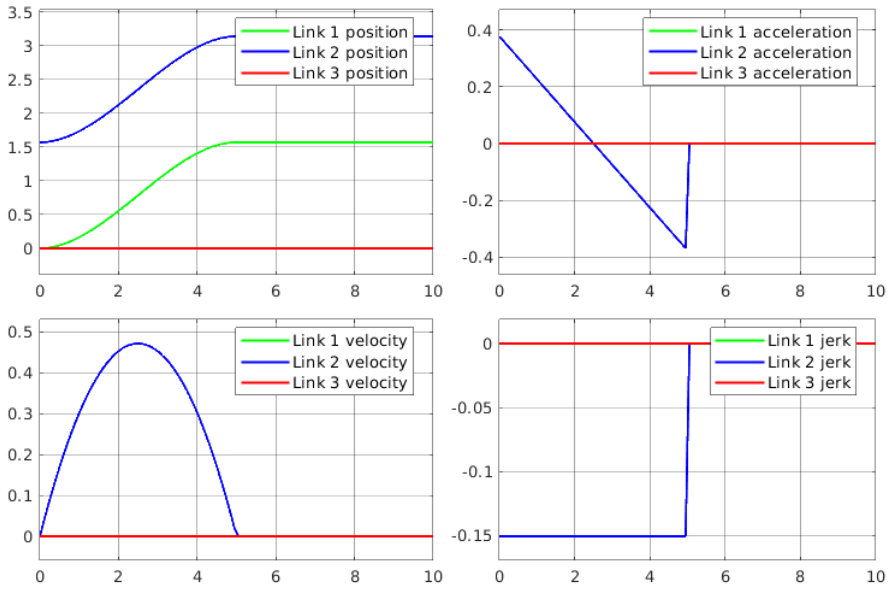

Figure 7: Plot of the desired trajectory for the 3R case.

Both the observers use the same set of 12 real eigenvalues equally spaced between $[-250; -260]$. Since the links' positions are available for measurement, we initialize, for the time being, the estimate of the links' positions of $\mathcal{O}_1$ and $\mathcal{O}_2$ with their available measurements at time zero, i.e.

$$\begin{bmatrix} \widehat{\mathbf{q}}_1^\top(0) & \widehat{\mathbf{q}}_2^\top(0) & \dot{\widehat{\mathbf{q}}}_1^\top(0) & \dot{\widehat{\mathbf{q}}}_2^\top(0) \end{bmatrix} = \begin{bmatrix} \mathbf{q}_1^\top(0) & 0 & 0 & 0 \end{bmatrix} \tag{5.3}$$

As mentioned above, such inizialization can be always done.

Simulation 3 In this simulation, we compare the behavior of $\mathcal{O}_1$ and $\mathcal{O}_2$. Both the observers are set as to have eigenvalues in $[-250; -260]$.
First of all let us focus on $\mathcal{O}_1$, the below plots show the time evolution of the errors of the links' and motors' positions and velocities.

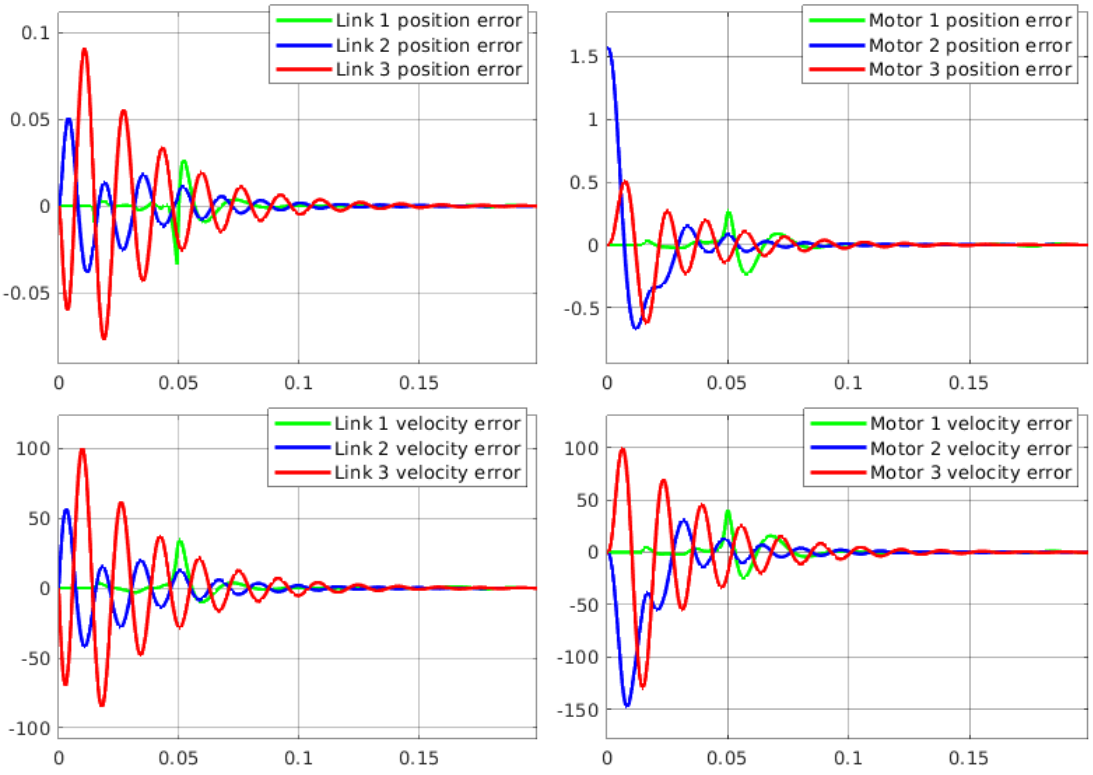

Figure 8: *Simulation 3.* Plot of the time evolution of the error for $\mathcal{O}_1$.

It is possible to see that the observer recontructs the state very rapidly, since the modes are chosen fast, with some oscillations. Smaller eigenvalues could be chosen but so that the conditions of claim 3.1 are satisfied. The bigger error is observed on the estimate of their velocities. Considering observer $\mathcal{O}_2$ in the same situation, as shown below, one can see a general improvement for the estimation error (as expected), a significantly faster speed of reconstruction and less oscillation.

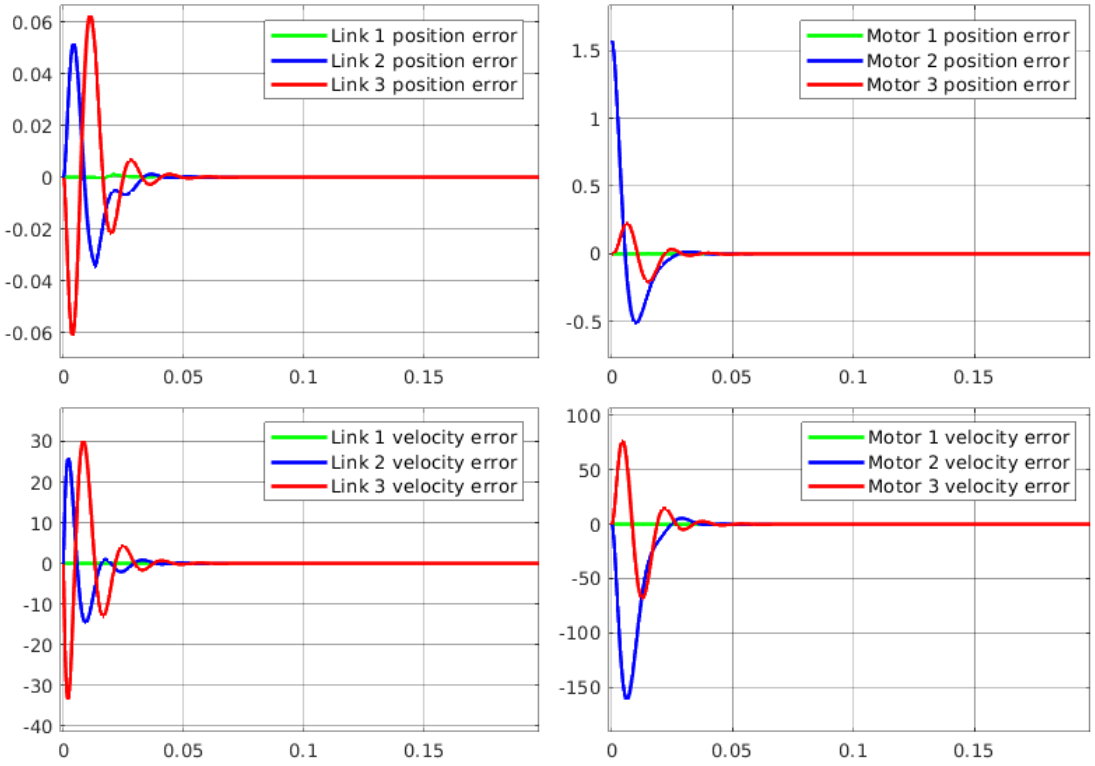

Figure 9: *Simulation 3.* Plot of the time evolution of the error for $\mathcal{O}_2$.

Simulation 4 In this simulation, by doubling the eigenvalues (now set to $[-500; -510]$), we observe less oscillation and overshoot, as shown in the following plots for $\mathcal{O}_1$. This behaviour is unusual since, for the choice of faster modes, one expects more oscillation and overshoot.

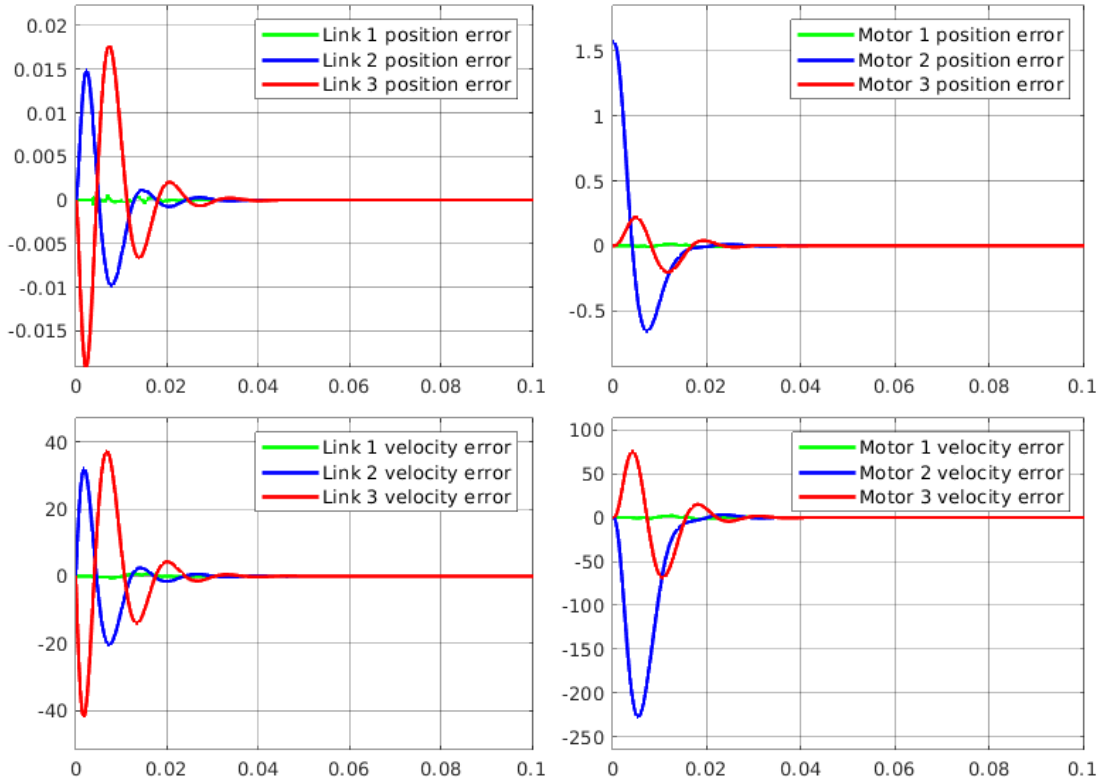

Figure 10: *Simulation 4*. Plot of the time evolution of the error for $\mathcal{O}_1$.

The behaviour of $\mathcal{O}_1$ with eigeinvalues in $[-500; -510]$ becomes closer to the one of $\mathcal{O}_2$ with eigeinvalues in $[-250; -260]$; it would seem that faster modes compensate in $\mathcal{O}_1$ for the lack of the links' velocites measurements.

Simulation 5 In this simulation, we want now to study a different scenario with respect to the previous one. We still command a rest to rest motion, but now starting from the initial configuration

$$\begin{bmatrix}\mathbf{q}_1^\top & \mathbf{q}_2^\top\end{bmatrix} = \begin{bmatrix}-\pi, \pi, -\pi & -\pi, \pi, -\pi\end{bmatrix}, \tag{5.4}$$

to the final one

$$\begin{bmatrix}\mathbf{q}_1^\top & \mathbf{q}_2^\top\end{bmatrix} = \begin{bmatrix}\frac{\pi}{2}, \pi, 0 & \frac{\pi}{2}, \pi, 0\end{bmatrix}. \tag{5.5}$$

The initial estimate of the observers is now set as:

$$\begin{bmatrix}\widehat{\mathbf{q}}_1(0)^\top & \dot{\widehat{\mathbf{q}}}_1(0)^\top & \widehat{\mathbf{q}}_2(0)^\top & \dot{\widehat{\mathbf{q}}}_2(0)^\top\end{bmatrix} = \begin{bmatrix}\mathbf{0}^\top & \mathbf{0}^\top & \mathbf{0}^\top & \mathbf{0}^\top\end{bmatrix}. \tag{5.6}$$

The idea is to set the observers with the highest possible initial error, since we assume that each joint/motor ranges in the interval $[-\pi; \pi]$ rad. Both the observers use the same set of 12 real eigenvalues equally spaced, in this case, between $[-85; -90]$. With such initializiation, we have started to experience some instability problems for $\mathcal{O}_1$ which is not able anymore to reconstruct the state of the system, as shown below.

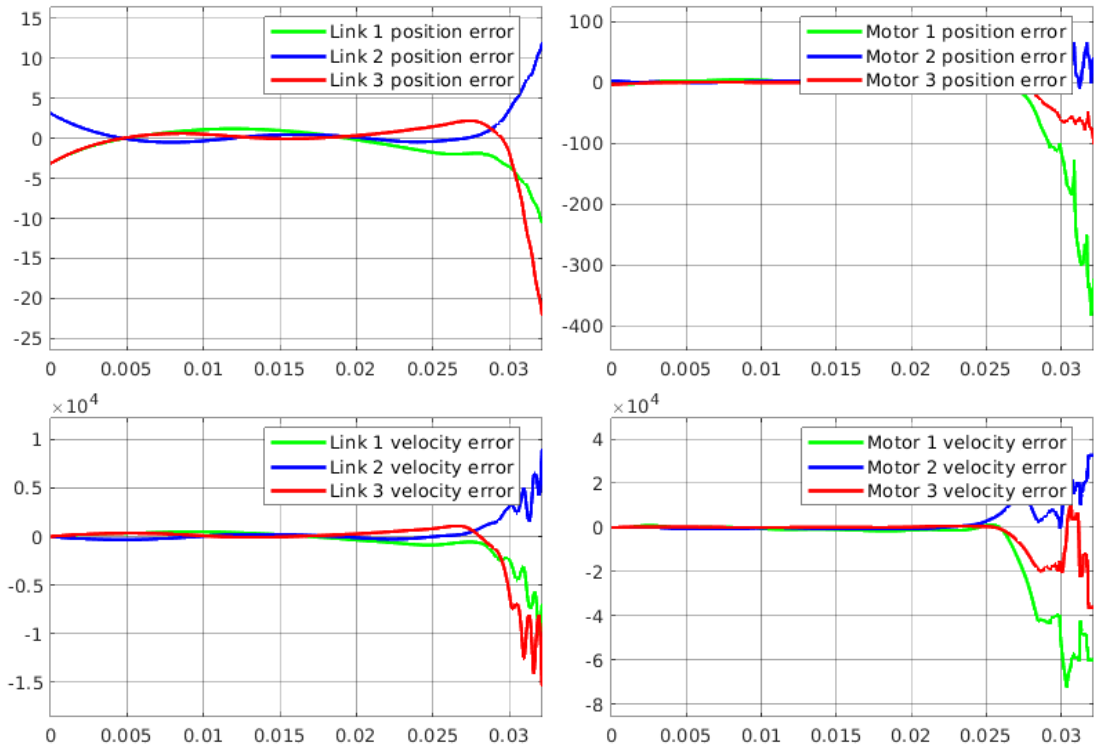

Figure 11: *Simulation 5.* Plot of the time evolution of the error for $\mathcal{O}_1$ using eigenvalues in $[-85; -90]$ with largest initial error.

Going in search of the cause of this instability, we first suspected some problems in the claims stated in section 3.2. Since $\mathcal{O}_1$ consists of a copy of the system with an additional corrective term driven by the error, we focused on the latter and in particular on the matrix $\mathbf{Q}(\mathbf{x})$. The requirement on $\mathbf{Q}(\mathbf{x})$ is quite simple, it has to be always nonsingular. Because simulations gave us a very small condition number for $\mathbf{Q}(\mathbf{x})$, we suspected that it could be singular for some configuarions. The determinant of $\mathbf{Q}(\mathbf{x})$, for the given dynamic parameters is:

$$\frac{15625000000000000000000000000000000}{\left(16\cos\left(q_3\right)^2 - 297\right)^2 \left(\cos\left(q_2+q_3\right)^2 + 8\,\cos\left(q_2+q_3\right)\,\cos\left(q_2\right) + 17\cos\left(q_2\right)^2 + 30\right)^2}, \tag{5.7}$$

which is clearly always different from 0, as expected from the theory. Thus we suspected (and still suspect) that the source of instability of $\mathcal{O}_1$ is purely numerical. This seems to be confirmed by the fact that by choosing smaller eigenvalues and thus, smaller gains, the error remains bounded but does not explode, as should be when the eigenvalues are chosen to slow. As a matter of fact, theoretically, faster modes should not cause the instability of the observer.
By these facts, it was decided to modify the observer so as to include a correction also on the basis of the links' velocity error, with the idea that a more robust behaviour would have been obtained.
Below one can see the time evolution of the error for the observer $\mathcal{O}_2$ in the same aforementioned situation for $\mathcal{O}_1$.

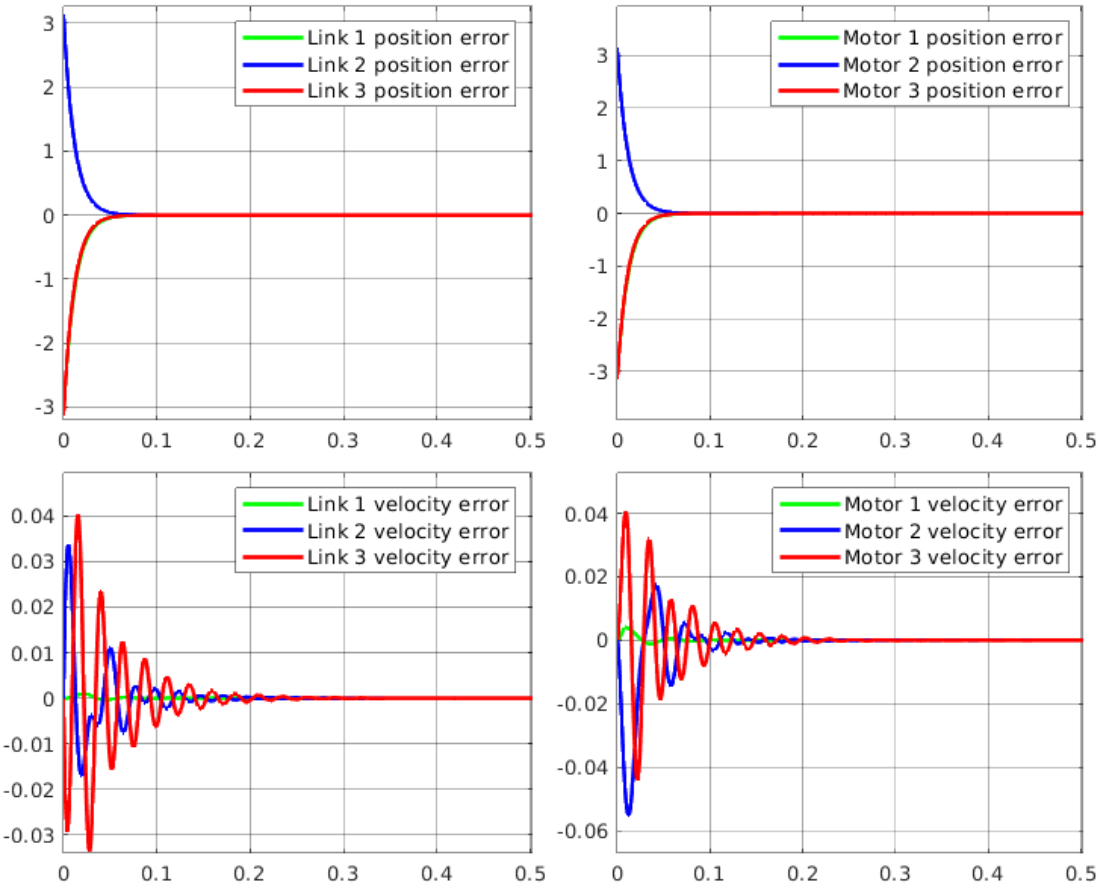

Figure 12: *Simulation 5.* Plot of the time evolution of the error for $\mathcal{O}_2$ using eigenvalues in $[-85; -90]$ with largest initial error.

$\mathcal{O}_2$ seems to be able to overcome the issues encountered by $\mathcal{O}_1$. By decreasing the eigenvalues of $\mathcal{O}_2$, we observed a permanent tracking error (as it happens for $\mathcal{O}_1$). On the other hand by increasing the eigenvalues, $\mathcal{O}_2$ behaves as expected; indeed it drives the error more rapidly to zero and remains stable, as we show in the next simulation.

Simulation 6 In this simulation, we observe the time evolution of the error of $\mathcal{O}_2$ when the initial state of the robot is:

$$\begin{bmatrix}\mathbf{q}_1^\top(0) & \mathbf{q}_2^\top(0) & \dot{\mathbf{q}}_1^\top(0) & \dot{\mathbf{q}}_2^\top(0)\end{bmatrix} = \begin{bmatrix}-\pi, \pi, -\pi & -1.5\pi, 0.5\pi, -\pi & -4, 5, 10 & 6, 10, -20\end{bmatrix}, \quad (5.8)$$

(which is a quite unlikely situation), the initial state of $\mathcal{O}_2$ is still zero and the eigenvalues are equally spaced in $[-250; -260]$.

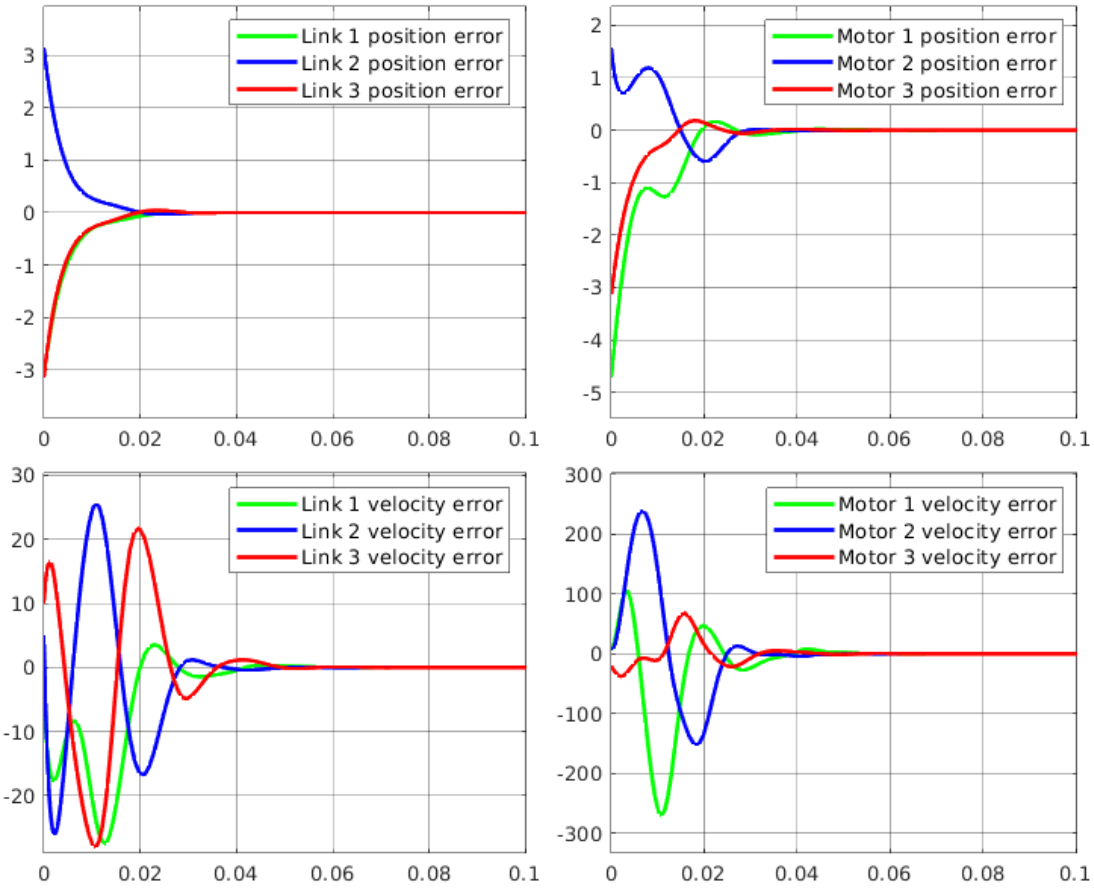

Figure 13: *Simulation 6.* Plot of the time evolution of the error for $\mathcal{O}_2$ using eigenvalues in $[-250; -260]$ starting from a very unlikely estimation error.

Thus we conclude that, even if it should always work, $\mathcal{O}_1$ is subject to instability when the estimate of the links' positions is not initialized using the available measurements. It seems that this problem can be overcomed assuming that also the links' velocities are available for measurement and modifying accordingly the gain of the observer.

Ciccarella-Germani with motors' positions and elastic torque As shown in section 3.2 by claim 3.6 it is also possible to implement an observer of the form (3.10) which uses, as measurements, the motors' positions and the elastic torque.

Simulation 7 In this simulation the robot starts from the initial configuration

$$\begin{bmatrix} \mathbf{q}_1^\top & \mathbf{q}_2^\top \end{bmatrix} = \begin{bmatrix} 0, \frac{\pi}{2}, 0 & 0, \frac{\pi}{2}, 0 \end{bmatrix} \tag{5.9}$$

with zero velocity. The observer described above, that will be denoted as $\mathcal{O}_3$, is inizialized with

$$\begin{bmatrix} \widehat{\mathbf{q}}_1(0)^\top & \dot{\widehat{\mathbf{q}}}_1(0)^\top & \widehat{\mathbf{q}}_2(0)^\top & \dot{\widehat{\mathbf{q}}}_2(0)^\top \end{bmatrix} = \begin{bmatrix} \mathbf{0}^\top & \mathbf{0}^\top & \mathbf{0}^\top & \mathbf{0}^\top \end{bmatrix} \tag{5.10}$$

The eigenvalues are equally spaced in $[-250; -260]$

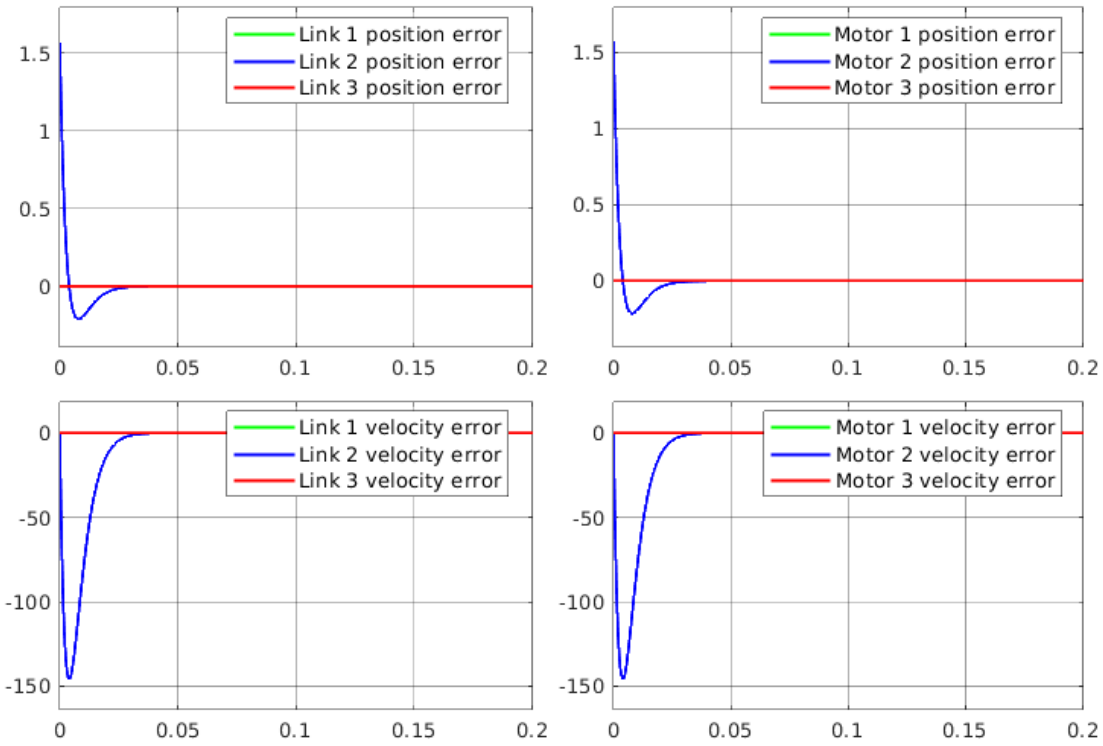

Figure 14: *Simulation 7.* Plot of the time evolution of the error for $\mathcal{O}_3$ using eigenvalues in $[-250; -260]$

Simulation 8 In this simulation with $\mathcal{O}_3$, the robot starts from the intial state

$$\begin{bmatrix}\mathbf{q}_1^\top(0) & \mathbf{q}_2^\top(0) & \dot{\mathbf{q}}_1^\top(0) & \dot{\mathbf{q}}_2^\top(0)\end{bmatrix} = \begin{bmatrix}-\pi, \pi, -\pi & -1.5\pi, 0.5\pi, -\pi & -4, 5, 10 & 6, 10, -20\end{bmatrix} \quad (5.11)$$

as in simulation 6. The inital state of $\mathcal{O}_3$ is still zero and the eigenvalues equally spaced in between $[-250; -260]$.

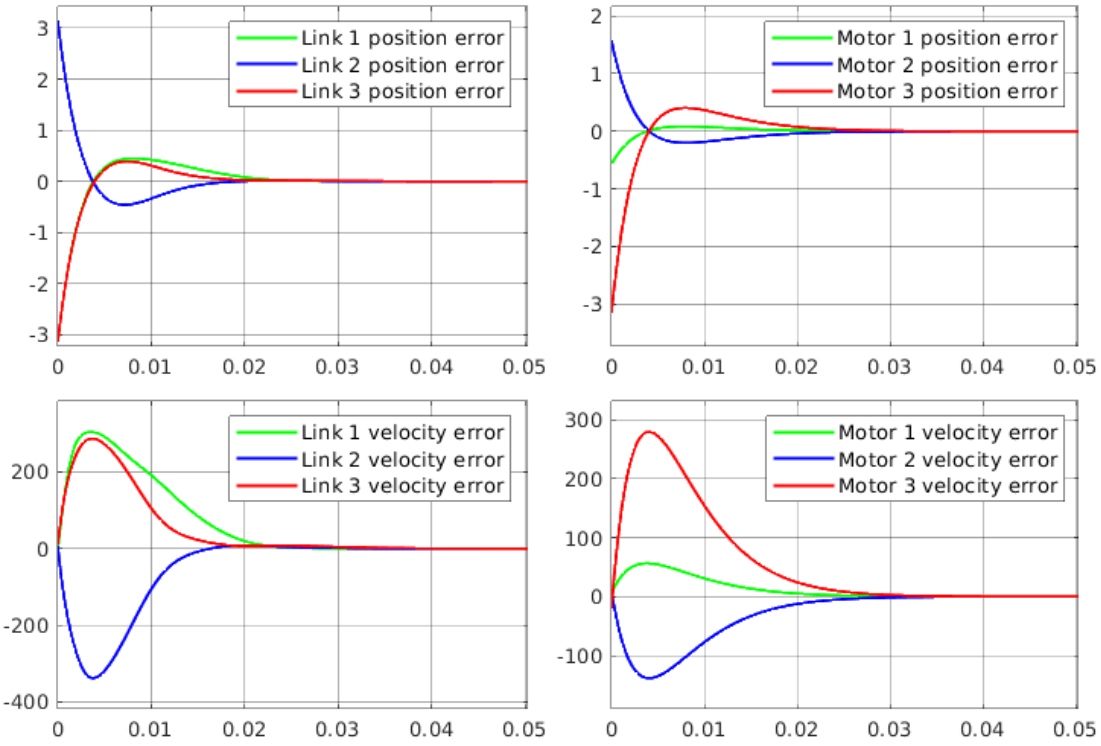

Figure 15: *Simulation 8.* Plot of the time evolution of the error for $\mathcal{O}_3$ using eigenvalues in $[-250; -260]$ in the same situation as simulation 6

$\mathcal{O}_3$ shows the same "robustenss" of $\mathcal{O}_2$. This is justified by the fact that it uses more measurements than $\mathcal{O}_1$ for reconstructing the state of the robot.

Ciccarella-Germani with only motors' positions Finally, we want to show the simulations performed using an observer of the form (3.10) which assumes as the output of the system only the motors' positions. For this observer, the asymptotic convergence of the error to zero is not guaranteed by the claims developed in section 3.2. Indeed with respect to the output $\mathbf{y} \triangleq \mathbf{x}_3 \in \mathbb{R}^n$ the vector relative degree of the system is only $\begin{bmatrix} r_1 & \cdots & r_n \end{bmatrix} = \begin{bmatrix} 2 & \cdots & 2 \end{bmatrix}$ so that $r_1 + \cdots + r_n = 2n$ and not $4n$ as it should be to satisfy claim 3.1. On the other hand, we have noticed that such observer seems to be able to reconstruct the state of the robot in all those situations where $\mathcal{O}_1$ succeeds and even in the "unlikely" cases considered for $\mathcal{O}_2$ and $\mathcal{O}_3$. Such observer will be denoted in the next with $\mathcal{O}_4$.

Simulation 9 In this simulation the initial state of the robot is:

$$\begin{bmatrix} \mathbf{q}_1^\top(0) & \mathbf{q}_2^\top(0) & \dot{\mathbf{q}}_1^\top(0) & \dot{\mathbf{q}}_2^\top(0) \end{bmatrix} = \begin{bmatrix} 0, \frac{\pi}{2}, 0 & 0, \frac{\pi}{2}, 0 & 0, 0, 0 & 0, 0, 0 \end{bmatrix}. \tag{5.12}$$

As usual, the initial state of $\mathcal{O}_4$ is zero and the eigenvalues are assigned in the interval $[-250; -260]$.

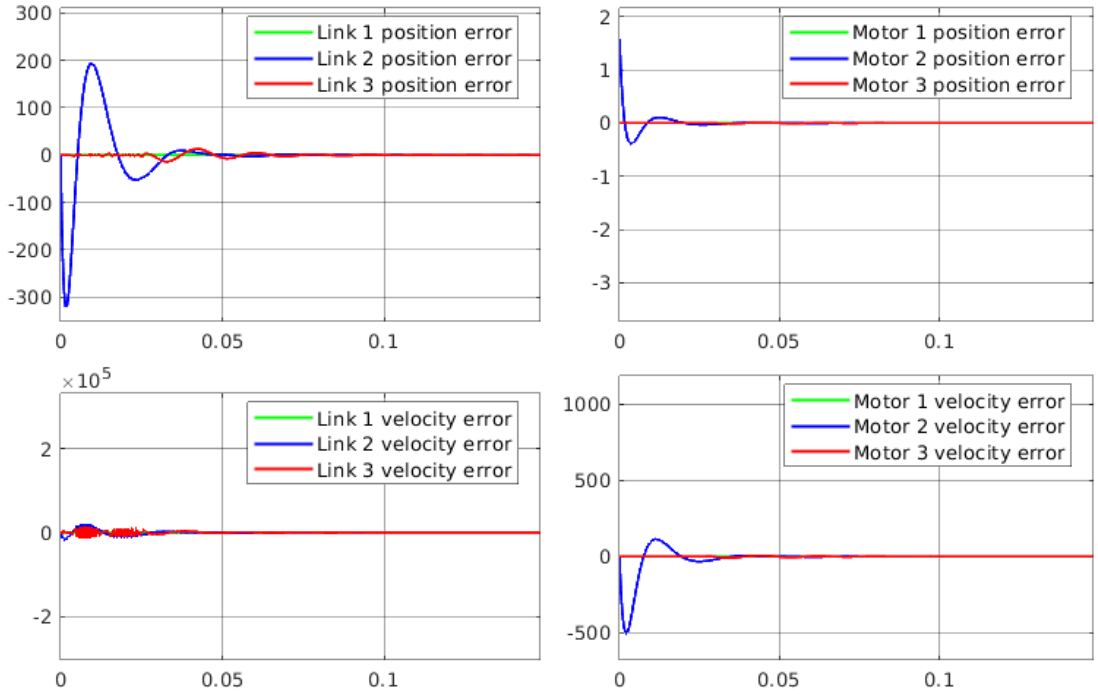

Figure 16: *Simulation 9.* Plot of the time evolution of the error for $\mathcal{O}_4$ using eigenvalues in $[-250; -260]$.

Simulation 10 In this simulation the initial state of the robot is:

$$\begin{bmatrix}\mathbf{q}_1^\top(0) & \mathbf{q}_2^\top(0) & \dot{\mathbf{q}}_1^\top(0) & \dot{\mathbf{q}}_2^\top(0)\end{bmatrix} = \begin{bmatrix}-\pi, \pi, -\pi & -1.5\pi, 0.5\pi, -\pi & -4, 5, 10 & 6, 10, -20\end{bmatrix}. \tag{5.13}$$

The initial state of $\mathcal{O}_4$ is zero and the eigenvalues are assigned in the interval $[-250; -260]$.

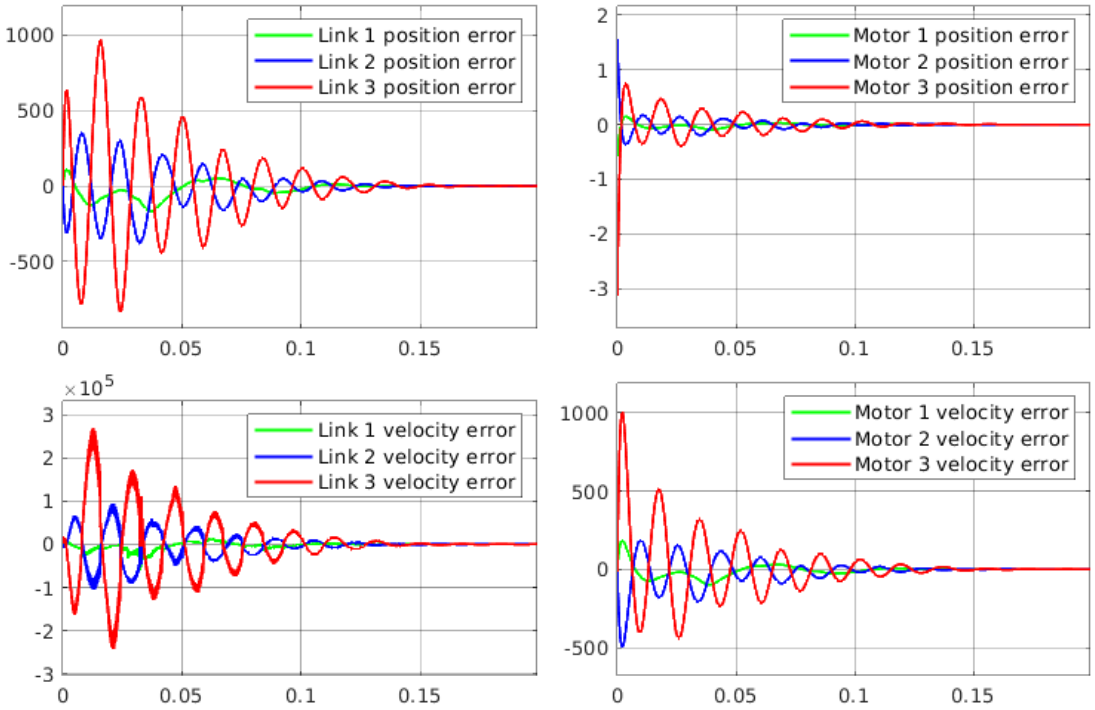

Figure 17: *Simulation 10.* Plot of the time evolution of the error for $\mathcal{O}_4$ using eigenvalues in $[-250; -260]$ in the same situation as simulation 6.

The error of $\mathcal{O}_4$ is very large but surprisingly it is able to reconstruct the whole state of the robot.

6 Conclusion

We would like to conclude this report by underlining some possibilities for future work on the project. In particular, although viscous friction has been neglected, it would be an easy addition to implement. Although we did not consider this scenario while performing the simulations, it would be interesting to study an observer following the structure of the one from Ciccarella-Germani but employing the motors' positions and links' accelerations; an observer using such measurements has been proposed in [5]. Then, it would be interesting to further investigate the instability of the Ciccarella-Germani observer and its source. Finally, following this investigation, one could perform a robustness analysis of this observer to assess its performance in the case of uncertainties of model parameters, something that has not been taken into consideration in this report.

A Proofs

Here we report the proofs of the theorems and claims stated throughout the document. The statements of the theorems are included as well, for the sake of clarity.

A.1 Extension to the MIMO systems

Consider a nonlinear (square) MIMO system of the form

$$\begin{aligned}\dot{\mathbf{x}} &= \mathbf{f}(\mathbf{x}) + \mathbf{G}(\mathbf{x})\mathbf{u} = \mathbf{f}(\mathbf{x}) + \sum_{i=1}^{m} g_i(\mathbf{x})u_i \\ \mathbf{y} &= \mathbf{H}(\mathbf{x}) = \begin{bmatrix} h_1(\mathbf{x}) \\ \vdots \\ h_m(\mathbf{x}) \end{bmatrix},\end{aligned} \tag{A.1}$$

where $\mathbf{x} \in \mathbb{R}^n$ is the state of the system, $\mathbf{u} \in \mathbb{R}^m$ is the input to the system and $\mathbf{y} \in \mathbb{R}^m$ is the output of the system. With reference to the results presented in [3], we want to generalize to the MIMO case Theorems 1 and 2 and the relative corollaries.

Theorem A.1 (Generalization of Theorem 1)**.** *Suppose to feed the system with an input* $\mathbf{u}(t) \equiv \mathbf{0}, \forall t \geq 0$*. Let* $L_{\mathbf{f}}^k \mathbf{h}(\mathbf{x})$ *be the k-th Lie derivative of the function* $\mathbf{h}$ *with respect to the vector field* $\mathbf{f}$*. If:*

(H1) There exists a collection of nonnegative integers $r_1, r_2, \ldots, r_m$ *such that* $dim(\mathbf{x}) = n = r_1 + r_2 + \cdots + r_m$ *and* $rank(\mathbf{Q}(\mathbf{x})) = n$ *where* $\mathbf{Q}(\mathbf{x})$ *is defined as*

$$\mathbf{Q}(\mathbf{x}) \triangleq \frac{\mathrm{d}}{\mathrm{d}\mathbf{x}} \left[\begin{array}{c} h_1 \\ \vdots \\ L_{\mathbf{f}}^{r_1-1} h_1 \\ \hline h_2 \\ \vdots \\ L_{\mathbf{f}}^{r_2-1} h_2 \\ \hline \vdots \\ \hline h_m \\ \vdots \\ L_{\mathbf{f}}^{r_m-1} h_m \end{array}\right]. \tag{A.2}$$

(H2) The vector

$$\left.\begin{pmatrix} L_{\mathbf{f}}^{r_1} h_1 \\ \vdots \\ L_{\mathbf{f}}^{r_m} h_m \end{pmatrix}\right|_{\mathbf{x}=\mathbf{\Phi}^{-1}(\mathbf{z})} \tag{A.3}$$

is uniformly Hölder, i.e.

$$\begin{aligned}&\forall \boldsymbol{\zeta}_1, \boldsymbol{\zeta}_2 \in \mathbb{R}^n \quad \exists \gamma > 0, \delta \in (0,1] \quad \textit{such that} \\ &\left\| \begin{bmatrix} L_{\mathbf{f}}^{r_1} h_1(\mathbf{\Phi}^{-1}(\boldsymbol{\zeta}_1)) - L_{\mathbf{f}}^{r_1} h_1(\mathbf{\Phi}^{-1}(\boldsymbol{\zeta}_2)) \\ \vdots \\ L_{\mathbf{f}}^{r_m} h_m(\mathbf{\Phi}^{-1}(\boldsymbol{\zeta}_1)) - L_{\mathbf{f}}^{r_1} h_1(\mathbf{\Phi}^{-1}(\boldsymbol{\zeta}_2)) \end{bmatrix} \right\|, \leq \gamma \|\boldsymbol{\zeta}_1 - \boldsymbol{\zeta}_2\|^{\delta}\end{aligned} \tag{A.4}$$

then, there exists a collection of finite gain vectors $\mathbf{K}_1 \in \mathbb{R}^{r_1}, \ldots, \mathbf{K}_m \in \mathbb{R}^{r_m}$ *such that the solution of the following system of equations (*the proposed observer*)*

$$\dot{\hat{\mathbf{x}}} = \mathbf{f}(\hat{\mathbf{x}}) + \mathbf{Q}(\hat{\mathbf{x}})^{-1} \begin{bmatrix} \mathbf{K}_1 & \mathbf{0} & \ldots & \mathbf{0} \\ \mathbf{0} & \mathbf{K}_2 & \ldots & \mathbf{0} \\ \vdots & \vdots & \ddots & \mathbf{0} \\ \mathbf{0} & \mathbf{0} & \ldots & \mathbf{K}_m \end{bmatrix} \begin{bmatrix} y_1 - h_1(\hat{\mathbf{x}}) \\ \vdots \\ y_m - h_m(\hat{\mathbf{x}}) \end{bmatrix} \tag{A.5}$$

has the following properties:

1. *When* $\delta \in (0,1)$*, for any* $\epsilon > 0$ *and any* $\hat{\mathbf{x}}(0) \in \mathbb{R}^n$ *we have*

$$\lim_{t\to\infty} \|\hat{\mathbf{x}}(t) - \mathbf{x}(t)\| \leq \epsilon. \tag{A.6}$$

2. *When* $\delta = 1$*, for any* $\hat{\mathbf{x}}(0) \in \mathbb{R}^n$ *we have*

$$\lim_{t\to\infty} \|\hat{\mathbf{x}}(t) - \mathbf{x}(t)\| = 0. \tag{A.7}$$

Proof. Consider the nonlinear change of coordinates

$$\mathbf{z} \triangleq \mathbf{\Phi}(\mathbf{x}) \triangleq \begin{bmatrix} h_1 \\ \vdots \\ L_{\mathbf{f}}^{r_1-1} h_1 \\ \hline h_2 \\ \vdots \\ L_{\mathbf{f}}^{r_2-1} h_2 \\ \hline \vdots \\ \hline h_m \\ \vdots \\ L_{\mathbf{f}}^{r_m-1} h_m \end{bmatrix}. \tag{A.8}$$

By hypothesis H1 and the inverse function theorem, $\mathbf{\Phi}(\mathbf{x})$ is a global diffeomorphism. Let us rewrite the system in the new coordinates:

$$\begin{aligned} z_1 = h_1 &\implies \dot{z}_1 = \frac{\partial h_1}{\partial \mathbf{x}} \dot{\mathbf{x}} = L_{\mathbf{f}} h_1 = z_2 \\ z_2 = L_{\mathbf{f}} h_1 &\implies \dot{z}_2 = \frac{\partial L_{\mathbf{f}} h_1}{\partial \mathbf{x}} \dot{x} = L_{\mathbf{f}}^2 h_1 = z_3 \\ &\vdots \\ z_{r_1-1} = L_{\mathbf{f}}^{r_1-2} h_1 &\implies \dot{z}_{r_1-1} = \frac{\partial L_{\mathbf{f}}^{r_1-2} h_1}{\partial \mathbf{x}} \dot{\mathbf{x}} = L_{\mathbf{f}}^{r_1-1} h_1 = z_{r_1} \\ z_{r_1} = L_{\mathbf{f}}^{r_1-1} h_1 &\implies \dot{z}_{r_1} = \frac{\partial L_{\mathbf{f}}^{r_1-1} h_1}{\partial \mathbf{x}} \dot{\mathbf{x}} \Big|_{\mathbf{x}=\mathbf{\Phi}^{-1}(\mathbf{z})} = L_{\mathbf{f}}^{r_1} h_1 \Big|_{x=\Phi^{-1}(z)}. \end{aligned} \tag{A.9}$$

Iterating this procedure for every r_i we get:

$$\dot{\mathbf{z}} = \begin{bmatrix} \mathbf{A}_1 & \mathbf{0} & \dots & \mathbf{0} \\ \mathbf{0} & \mathbf{A}_2 & \dots & \mathbf{0} \\ \vdots & \vdots & \ddots & \vdots \\ \mathbf{0} & \mathbf{0} & \dots & \mathbf{A}_m \end{bmatrix} \mathbf{z} + \left. \begin{bmatrix} \mathbf{B}_1 L_{\mathbf{f}}^{r_1} h_1 \\ \mathbf{B}_2 L_{\mathbf{f}}^{r_2} h_2 \\ \vdots \\ \mathbf{B}_m L_{\mathbf{f}}^{r_m} h_m \end{bmatrix} \right|_{\mathbf{x}=\mathbf{\Phi}^{-1}(\mathbf{z})} \tag{A.10}$$

$$\mathbf{y} = \begin{bmatrix} \mathbf{C}_1 & \mathbf{0} & \dots & \mathbf{0} \\ \mathbf{0} & \mathbf{C}_2 & \dots & \mathbf{0} \\ \vdots & \vdots & \ddots & \vdots \\ \mathbf{0} & \mathbf{0} & \dots & \mathbf{C}_m \end{bmatrix} \mathbf{z}, \tag{A.11}$$

where, since $\mathbf{A}_i \in \mathbb{R}^{r_i \times r_i}, \mathbf{B}_i \in \mathbb{R}^{r_i \times 1}, \mathbf{C}_i \in \mathbb{R}^{1 \times r_i}$ are state, input and output matrices in the *Brunowski* form, the pair $\mathbf{A} \triangleq diag\{\mathbf{A}_1, \dots, \mathbf{A}_m\}, \mathbf{C} \triangleq diag\{\mathbf{C}_1, \dots, \mathbf{C}_m\}$ is observable. Applying the same change of coordinates to the proposed observer we get

$$\begin{aligned} \dot{\hat{\mathbf{z}}} &= \begin{bmatrix} \mathbf{A}_1 & \mathbf{0} & \dots & \mathbf{0} \\ 0 & \mathbf{A}_2 & \dots & \mathbf{0} \\ \vdots & \vdots & \ddots & \vdots \\ \mathbf{0} & \mathbf{0} & \dots & \mathbf{A}_m \end{bmatrix} \hat{\mathbf{z}} + \left. \begin{bmatrix} \mathbf{B}_1 L_{\mathbf{f}}^{r_1} h_1 \\ \mathbf{B}_2 L_{\mathbf{f}}^{r_2} h_2 \\ \vdots \\ \mathbf{B}_m L_{\mathbf{f}}^{r_m} h_m \end{bmatrix} \right|_{\mathbf{x}=\mathbf{\Phi}^{-1}(\hat{\mathbf{z}})} + \begin{bmatrix} \mathbf{K}_1 & \mathbf{0} & \dots & \mathbf{0} \\ \mathbf{0} & \mathbf{K}_2 & \dots & \mathbf{0} \\ \vdots & \vdots & \ddots & \vdots \\ \mathbf{0} & \mathbf{0} & \dots & \mathbf{K}_m \end{bmatrix} (\mathbf{y} - \mathbf{C}\hat{\mathbf{z}}) \\ &= (\mathbf{A} - \mathbf{KC})\,\hat{\mathbf{z}} + \left. \begin{bmatrix} \mathbf{B}_1 L_{\mathbf{f}}^{r_1} h_1 \\ \mathbf{B}_2 L_{\mathbf{f}}^{r_2} h_2 \\ \vdots \\ \mathbf{B}_m L_{\mathbf{f}}^{r_m} h_m \end{bmatrix} \right|_{\mathbf{x}=\mathbf{\Phi}^{-1}(\hat{\mathbf{z}})} + \mathbf{K}\mathbf{y} \end{aligned} \tag{A.12}$$

$$\mathbf{y} = \begin{bmatrix} \mathbf{C}_1 & \mathbf{0} & \dots & \mathbf{0} \\ \mathbf{0} & \mathbf{C}_2 & \dots & \mathbf{0} \\ \vdots & \vdots & \ddots & \vdots \\ \mathbf{0} & \mathbf{0} & \dots & \mathbf{C}_m \end{bmatrix} \mathbf{z}. \tag{A.13}$$

Now, consider the *estimation error* $\boldsymbol{\xi}(t) \triangleq \hat{\mathbf{z}}(t) - \mathbf{z}(t)$; its dynamics is:

$$\begin{aligned} \dot{\boldsymbol{\xi}} &= \dot{\hat{\mathbf{z}}} - \dot{\mathbf{z}} \\ &= (\mathbf{A} - \mathbf{KC})\hat{\mathbf{z}} + \left. \begin{bmatrix} \mathbf{B}_1 L_{\mathbf{f}}^{r_1} h_1 \\ \mathbf{B}_2 L_{\mathbf{f}}^{r_2} h_2 \\ \vdots \\ \mathbf{B}_m L_{\mathbf{f}}^{r_m} h_m \end{bmatrix} \right|_{\mathbf{x}=\mathbf{\Phi}^{-1}(\hat{\mathbf{z}})} + \mathbf{K}\mathbf{y} - \mathbf{A}\mathbf{z} - \left. \begin{bmatrix} \mathbf{B}_1 L_{\mathbf{f}}^{r_1} h_1 \\ \mathbf{B}_2 L_{\mathbf{f}}^{r_2} h_2 \\ \vdots \\ \mathbf{B}_m L_{\mathbf{f}}^{r_m} h_m \end{bmatrix} \right|_{\mathbf{x}=\mathbf{\Phi}^{-1}(\mathbf{z})} \\ &= (\mathbf{A} - \mathbf{KC})\boldsymbol{\xi} + \underbrace{\begin{bmatrix} \mathbf{B}_1 & \mathbf{0} & \dots & \mathbf{0} \\ \mathbf{0} & \mathbf{B}_2 & \dots & \mathbf{0} \\ \vdots & \vdots & \ddots & \vdots \\ \mathbf{0} & \mathbf{0} & \dots & \mathbf{B}_m \end{bmatrix}}_{\triangleq \mathbf{B}} \begin{bmatrix} L_{\mathbf{f}}^{r_1} h_1(\mathbf{\Phi}^{-1}(\hat{\mathbf{z}})) - L_{\mathbf{f}}^{r_1} h_1(\mathbf{\Phi}^{-1}(\mathbf{z})) \\ \vdots \\ L_{\mathbf{f}}^{r_m} \underbrace{h_m(\mathbf{\Phi}^{-1}(\hat{\mathbf{z}}))}_{\hat{h}_m} - L_{\mathbf{f}}^{r_1} h_1(\mathbf{\Phi}^{-1}(\mathbf{z})) \end{bmatrix}. \end{aligned} \tag{A.14}$$

Let $\mathbf{V}(\boldsymbol{\lambda}) \triangleq diag\{\mathbf{V}_1(\boldsymbol{\lambda}), \dots, \mathbf{V}_m(\boldsymbol{\lambda})\}$ where $\mathbf{V}_i(\boldsymbol{\lambda})$ is the Vandermonde matrix that diagonalizes the companion matrix $(\mathbf{A}_i - \mathbf{K}_i\mathbf{C}_i), i = 1, \dots, m$. Thus we have

$$e^{(\mathbf{A}-\mathbf{KC})t} = \mathbf{V}^{-1}(\boldsymbol{\lambda}) e^{\mathbf{\Lambda} t} \mathbf{V}(\boldsymbol{\lambda}) \tag{A.15}$$

and we can write

$$\begin{aligned}\boldsymbol{\xi}(t) &= e^{(\mathbf{A}-\mathbf{KC})t}\boldsymbol{\xi}(0) + \int_0^\top e^{(\mathbf{A}-\mathbf{KC})(t-\tau)}\mathbf{B}\begin{bmatrix} L_{\mathbf{f}}^{r_1}\hat{h}_1 - L_{\mathbf{f}}^{r_1}h_1 \\ \vdots \\ L_{\mathbf{f}}^{r_m}\hat{h}_m - L_{\mathbf{f}}^{r_1}h_1 \end{bmatrix} d\tau \\ \mathbf{V}(\boldsymbol{\lambda})\boldsymbol{\xi}(t) &= e^{\Lambda t}\mathbf{V}(\boldsymbol{\lambda})\boldsymbol{\xi}(0) + \int_0^\top e^{\mathbf{\Lambda}(t-\tau)}\mathbf{V}(\boldsymbol{\lambda})B\begin{bmatrix} L_{\mathbf{f}}^{r_1}\hat{h}_1 - L_{\mathbf{f}}^{r_1}h_1 \\ \vdots \\ L_{\mathbf{f}}^{r_m}\hat{h}_m - L_{\mathbf{f}}^{r_1}h_1 \end{bmatrix} d\tau.\end{aligned} \tag{A.16}$$

Now, notice that by the structures of the Vandermonde matrix and of the $\mathbf{B}$ matrix, the matrix $\mathbf{V}(\boldsymbol{\lambda})\mathbf{B}$ has the following form

$$\left(\begin{array}{cccc} 1 & 0 & \dots & 0 \\ \vdots & \vdots & \ddots & \vdots \\ 1 & 0 & \dots & 0 \\ \hline 0 & 1 & \dots & 0 \\ \vdots & \vdots & \ddots & \vdots \\ 0 & 1 & \dots & 0 \\ \hline & \vdots & \vdots & \\ \hline 0 & 0 & \dots & 1 \\ \vdots & \vdots & \ddots & \vdots \\ 0 & 0 & \dots & 1 \end{array}\right), \tag{A.17}$$

so that the matrix $(\mathbf{V}(\boldsymbol{\lambda})\mathbf{B})^\top(\mathbf{V}(\boldsymbol{\lambda})\mathbf{B})$ has the form

$$\begin{bmatrix} r_1 & 0 & \dots & 0 \\ 0 & r_2 & \dots & 0 \\ \vdots & \vdots & \ddots & 0 \\ 0 & 0 & \dots & r_m \end{bmatrix}, \tag{A.18}$$

thus we can write

$$\|\mathbf{V}(\boldsymbol{\lambda})\mathbf{B}\| = \sqrt{\lambda_{max}(\mathbf{V}(\boldsymbol{\lambda})\mathbf{B})^\top(\mathbf{V}(\boldsymbol{\lambda})\mathbf{B})} = \sqrt{r_{max}}, \quad r_{max} \triangleq \max\{r_1, \dots, r_m\}. \tag{A.19}$$

Notice that since $r_i \leq n$, surely $r_{max} \leq n$ therefore $\|\mathbf{V}(\boldsymbol{\lambda})\mathbf{B})\| \leq \sqrt{n}$.
Now, since the pair $(\mathbf{A}, \mathbf{C})$ is observable we can suitably compute $\mathbf{K}$ as to place the poles λ_i of $\mathbf{A} - \mathbf{KC}$ such that $\lambda_n < \lambda_{n-1} < \cdots < \lambda_1 < 0$. By the considerations above and by H2 we can

transform the (A.16) into the following inequality

$$\begin{aligned}
\|\mathbf{V}(\boldsymbol{\lambda})\boldsymbol{\xi}(t)\| &\leq \|\mathbf{V}(\boldsymbol{\lambda})\boldsymbol{\xi}(0)\|e^{\lambda_1 t} + \int_0^\top \|\mathbf{V}(\boldsymbol{\lambda})\mathbf{B}\|e^{\lambda_1(t-\tau)} \left\| \begin{bmatrix} L_{\mathbf{f}}^{r_1}\hat{h}_1 - L_{\mathbf{f}}^{r_1}h_1 \\ \vdots \\ L_{\mathbf{f}}^{r_m}\hat{h}_m - L_{\mathbf{f}}^{r_1}h_1 \end{bmatrix} \right\| d\tau \\
&\leq \|\mathbf{V}(\boldsymbol{\lambda})\boldsymbol{\xi}(0)\|e^{\lambda_1 t} + \int_0^\top \sqrt{n}e^{\lambda_1(t-\tau)} \left\| \begin{bmatrix} L_{\mathbf{f}}^{r_1}\hat{h}_1 - L_{\mathbf{f}}^{r_1}h_1 \\ \vdots \\ L_{\mathbf{f}}^{r_m}\hat{h}_m - L_{\mathbf{f}}^{r_1}h_1 \end{bmatrix} \right\| d\tau \\
&\leq \|\mathbf{V}(\boldsymbol{\lambda})\boldsymbol{\xi}(0)\|e^{\lambda_1 t} + \int_0^\top \sqrt{n}e^{\lambda_1(t-\tau)}\gamma\|\hat{\mathbf{z}}(\tau) - \mathbf{z}(\tau)\|^\delta d\tau \\
&\leq \|\mathbf{V}(\boldsymbol{\lambda})\boldsymbol{\xi}(0)\|e^{\lambda_1 t} + \int_0^\top \sqrt{n}e^{\lambda_1(t-\tau)}\gamma\|\boldsymbol{\xi}(\tau)\|^\delta d\tau \\
&\leq \|\mathbf{V}(\boldsymbol{\lambda})\boldsymbol{\xi}(0)\|e^{\lambda_1 t} + \int_0^\top \sqrt{n}e^{\lambda_1(t-\tau)}\gamma\left\|\mathbf{V}(\boldsymbol{\lambda})^{-1}\mathbf{V}(\boldsymbol{\lambda})\boldsymbol{\xi}(\tau)\right\|^\delta d\tau \\
&\leq \|\mathbf{V}(\boldsymbol{\lambda})\boldsymbol{\xi}(0)\|e^{\lambda_1 t} + \int_0^\top \sqrt{n}e^{\lambda_1(t-\tau)}\gamma\left\|\mathbf{V}(\boldsymbol{\lambda})^{-1}\right\|^\delta \|\mathbf{V}(\boldsymbol{\lambda})\boldsymbol{\xi}(\tau)\|^\delta d\tau.
\end{aligned} \tag{A.20}$$

Now, with the same arguments used in [3] the proof is completed. □

Remark A.1. Using similar considerations, it is possible to extend also Corollary 1 of [3].

Theorem A.2 (Generalization of Theorem 2)**.** *Suppose system* (A.1) *has vector relative degree* $\mathbf{r} = \begin{bmatrix} r_1, \dots, r_m \end{bmatrix}^\top$ *such that* $r_1 + \cdots + r_m = n$*. Let* $\mathbf{U}(\mathbf{x})$ *be the* decoupling matrix *[4] of the system:*

$$\mathbf{U}(\mathbf{x}) = \begin{bmatrix} L_{g_1}L_f^{r_1-1}h_1 & \dots & L_{g_m}L_f^{r_1-1}h_1 \\ \vdots & \ddots & \vdots \\ L_{g_1}L_f^{r_m-1}h_m & \dots & L_{g_m}L_f^{r_m-1}h_m \end{bmatrix}, \tag{A.21}$$

and let $\mathbf{Q}(\mathbf{x})$ *be the same as in* (A.2)*. If*

(H1) $rank(\mathbf{Q}(\mathbf{x})) = n$*.*

(H2) The vector

$$\begin{bmatrix} L_{\mathbf{f}}^{r_1}h_1(\boldsymbol{\Phi}^{-1}(\mathbf{z})) \\ \vdots \\ L_{\mathbf{f}}^{r_m}h_m(\boldsymbol{\Phi}^{-1}(\mathbf{z})) \end{bmatrix} + \mathbf{U}(\boldsymbol{\Phi}^{-1}(\mathbf{z}))\mathbf{u} \tag{A.22}$$

is uniformly Hölder for all bounded inputs $\mathbf{u}$*, i.e.*

$$\begin{gathered}
\forall \zeta_1, \boldsymbol{\zeta}_2 \in \mathbb{R}^n \quad \exists \gamma > 0, \delta \in (0,1] \quad \textit{such that} \\
\sup_{\|\mathbf{u}\| \leq M} \left\| \left(\begin{bmatrix} L_{\mathbf{f}}^{r_1}h_1(\boldsymbol{\Phi}^{-1}(\boldsymbol{\zeta}_1)) \\ \vdots \\ L_{\mathbf{f}}^{r_m}h_m(\boldsymbol{\Phi}^{-1}(\boldsymbol{\zeta}_1)) \end{bmatrix} + \mathbf{U}(\boldsymbol{\Phi}^{-1}(\boldsymbol{\zeta}_1))\mathbf{u} \right) - \left(\begin{bmatrix} L_{\mathbf{f}}^{r_1}h_1(\boldsymbol{\Phi}^{-1}(\boldsymbol{\zeta}_2)) \\ \vdots \\ L_{\mathbf{f}}^{r_m}h_m(\boldsymbol{\Phi}^{-1}(\boldsymbol{\zeta}_2)) \end{bmatrix} + \mathbf{U}(\boldsymbol{\Phi}^{-1}(\boldsymbol{\zeta}_2))\mathbf{u} \right) \right\| \\
\leq \gamma\|\boldsymbol{\zeta}_1 - \boldsymbol{\zeta}_2\|^\delta
\end{gathered} \tag{A.23}$$

then there exists a collection of finite gain vectors $K_1 \in \mathbb{R}^{r_1}, \dots, K_m \in \mathbb{R}^{r_m}$ *such that the following system of equations (*the proposed observer modified for the system with nonzero input*)*

$$\dot{\hat{\mathbf{x}}} = \mathbf{f}(\hat{\mathbf{x}}) + \mathbf{G}(\hat{\mathbf{x}})\mathbf{u} + \mathbf{Q}(\hat{\mathbf{x}})^{-1} \begin{bmatrix} \mathbf{K}_1 & \mathbf{0} & \dots & \mathbf{0} \\ \mathbf{0} & \mathbf{K}_2 & \dots & \mathbf{0} \\ \vdots & \vdots & \ddots & \mathbf{0} \\ \mathbf{0} & \mathbf{0} & \dots & \mathbf{K}_m \end{bmatrix} (\mathbf{y} - \mathbf{H}(\hat{\mathbf{x}})) \tag{A.24}$$

has the following properties:

1. *When* $\delta \in (0,1)$*, for any* $\epsilon > 0, \hat{\mathbf{x}}(0) \in \mathbb{R}^n$ *we have*

$$\lim_{t\to\infty} \|\hat{\mathbf{x}}(t) - \mathbf{x}(t)\| \leq \epsilon. \tag{A.25}$$

2. *When* $\delta = 1$*, for any* $\hat{\mathbf{x}}(0) \in \mathbb{R}^n$ *we have*

$$\lim_{t\to\infty} \|\hat{\mathbf{x}}(t) - \mathbf{x}(t)\| = 0. \tag{A.26}$$

Proof. The proof proceeds in a similar way as before. Considering the same change of coordinates $\mathbf{z} = \mathbf{\Phi}(\mathbf{x})$ as in (A.8), we have

$$\begin{aligned}
\dot{z}_1 &= \frac{\partial h_1}{\partial \mathbf{x}}\dot{\mathbf{x}} = \frac{\partial h_1}{\partial \mathbf{x}} \left(\mathbf{f}(\mathbf{x}) + g_1(\mathbf{x})u_1 + \dots + g_m(\mathbf{x})u_m\right) \\
&= L_{\mathbf{f}}h_1 + (L_{g_1}h_1)u_1 + \dots + (L_{g_m}h_m)u_m \underbrace{=}_{\text{by assumption of vector relative degree}} L_{\mathbf{f}}h_1 = z_2 \\
\dot{z}_2 &= \dots = z_3 \\
&\vdots \\
\dot{z}_{r_1-1} &= z_{r_1} \\
\dot{z}_{r_1} &= \frac{\partial L_{\mathbf{f}}^{r_1-1}h_1}{\partial \mathbf{x}}\dot{\mathbf{x}} = \frac{\partial L_{\mathbf{f}}^{r_1-1}h_1}{\partial \mathbf{x}} \left(\mathbf{f}(\mathbf{x}) + g_1(\mathbf{x})u_1 + \dots g_m(\mathbf{x})u_m\right) \\
&= L_{\mathbf{f}}^{r_1}h_1\Big|_{\mathbf{x}=\mathbf{\Phi}^{-1}(\mathbf{z})} + \underbrace{\left[L_{g_1}L_{\mathbf{f}}^{r_1-1}h_1 \quad \dots \quad L_{g_m}L_{\mathbf{f}}^{r_1-1}\right]\Big|_{\mathbf{x}=\mathbf{\Phi}^{-1}(\mathbf{z})}}_{\text{First row of the decoupling matrix}} \mathbf{u}
\end{aligned} \tag{A.27}$$

Iterating this procedure for all the other components we get

$$\begin{aligned}
\dot{\mathbf{z}} &= \mathbf{A}\mathbf{z} + \mathbf{B}\left(\begin{bmatrix} L_{\mathbf{f}}^{r_1}h_1 \\ \vdots \\ L_{\mathbf{f}}^{r_m}h_m \end{bmatrix}\Bigg|_{\mathbf{x}=\mathbf{\Phi}^{-1}(\mathbf{z})} + \begin{bmatrix} \mathbf{U}_{r_1}\mathbf{u} \\ \vdots \\ \mathbf{U}_{r_m}\mathbf{u} \end{bmatrix}\Bigg|_{x=\mathbf{\Phi}^{-1}(\mathbf{z})}\right) \\
&= \mathbf{A}\mathbf{z} + \mathbf{B}\left(\begin{bmatrix} L_{\mathbf{f}}^{r_1}h_1 \\ \vdots \\ L_{\mathbf{f}}^{r_m}h_m \end{bmatrix}\Bigg|_{\mathbf{x}=\mathbf{\Phi}^{-1}(\mathbf{z})} + \mathbf{U}\Big|_{\mathbf{x}=\mathbf{\Phi}^{-1}(\mathbf{z})}\mathbf{u}\right)
\end{aligned} \tag{A.28}$$

$$\mathbf{y} = \mathbf{C}\mathbf{z} \tag{A.29}$$

where we have defined $\mathbf{A} = diag\{\mathbf{A}_1, \dots, \mathbf{A}_m\}$, $\mathbf{B} = diag\{\mathbf{B}_1, \dots, \mathbf{B}_m\}$, $\mathbf{C} = diag\{\mathbf{C}_1, \dots, \mathbf{C}_m\}$, and as before $\mathbf{A}_i \in \mathbb{R}^{r_i \times r_i}$, $\mathbf{B}_i \in \mathbb{R}^{r_i \times 1}$, $\mathbf{C}_i \in \mathbb{R}^{1 \times r_i}$ are the matrices in the *Brunowski* form.

Applying the same nonlinear change of variables to the observer we get

$$\begin{aligned}\dot{\hat{\mathbf{z}}} &= \mathbf{A}\hat{\mathbf{z}} + \mathbf{B}\left(\left.\begin{bmatrix} L_{\mathbf{f}}^{r_1}h_1 \\ \vdots \\ L_{\mathbf{f}}^{r_m}h_m \end{bmatrix}\right|_{\mathbf{x}=\mathbf{\Phi}^{-1}(\hat{\mathbf{z}})} + \mathbf{U}\Big|_{\mathbf{x}=\mathbf{\Phi}^{-1}(\hat{\mathbf{z}})}\mathbf{u}\right) + \mathbf{K}\left(\mathbf{y} - \mathbf{C}\hat{\mathbf{z}}\right) \\ &= (\mathbf{A} - \mathbf{KC})\hat{\mathbf{z}} + \mathbf{B}\left(\left.\begin{bmatrix} L_{\mathbf{f}}^{r_1}h_1 \\ \vdots \\ L_{\mathbf{f}}^{r_m}h_m \end{bmatrix}\right|_{\mathbf{x}=\mathbf{\Phi}^{-1}(\hat{\mathbf{z}})} + \mathbf{U}\Big|_{\mathbf{x}=\mathbf{\Phi}^{-1}(\hat{\mathbf{z}})}\mathbf{u}\right) + \mathbf{K}\mathbf{y}\end{aligned} \tag{A.30}$$

The estimation error is $\boldsymbol{\xi}(t) = \hat{\mathbf{z}}(t) - \mathbf{z}(t)$ and has dynamics:

$$\begin{aligned}\dot{\boldsymbol{\xi}} &= \dot{\hat{\mathbf{z}}} - \dot{\mathbf{z}} \\ &= (\mathbf{A} - \mathbf{KC})\xi + \mathbf{B}\left(\begin{bmatrix} L_{\mathbf{f}}^{r_1}\hat{h}_1 - L_{\mathbf{f}}^{r_1}h_1 \\ \vdots \\ L_{\mathbf{f}}^{r_m}\hat{h}_m - L_{\mathbf{f}}^{r_m}h_m \end{bmatrix} + (\hat{\mathbf{U}} - \mathbf{U})\mathbf{u}\right).\end{aligned} \tag{A.31}$$

Using the same arguments as before we can write

$$\mathbf{V}(\boldsymbol{\lambda})\boldsymbol{\xi}(t) = e^{\Lambda t}\mathbf{V}(\boldsymbol{\lambda})\boldsymbol{\xi}(0) + \int_0^\top e^{\Lambda(t-\tau)}\mathbf{V}(\boldsymbol{\lambda})\mathbf{B}\left(\begin{bmatrix} L_{\mathbf{f}}^{r_1}\hat{h}_1 - L_{\mathbf{f}}^{r_1}h_1 \\ \vdots \\ L_{\mathbf{f}}^{r_m}\hat{h}_m - L_{\mathbf{f}}^{r_m}h_m \end{bmatrix} + (\hat{\mathbf{U}} - \mathbf{U})\mathbf{u}\right)d\tau. \tag{A.32}$$

Moreover, with the usual manipulations, it is possible to write

$$\|\mathbf{V}(\boldsymbol{\lambda})\boldsymbol{\xi}(t)\| \leq \|\mathbf{V}(\boldsymbol{\lambda})\boldsymbol{\xi}(0)\| + \int_0^\top e^{\lambda_1(t-\tau)}\sqrt{n}\left\|\begin{bmatrix} L_{\mathbf{f}}^{r_1}\hat{h}_1 - L_{\mathbf{f}}^{r_1}h_1 \\ \vdots \\ L_{\mathbf{f}}^{r_m}\hat{h}_m - L_{\mathbf{f}}^{r_m}h_m \end{bmatrix} + (\hat{\mathbf{U}} - \mathbf{U})\mathbf{u}\right\|d\tau \tag{A.33}$$

and by H2 we can write

$$\begin{aligned}\|\mathbf{V}(\boldsymbol{\lambda})\boldsymbol{\xi}(t)\| &\leq \|\mathbf{V}(\boldsymbol{\lambda})\boldsymbol{\xi}(0)\| + \int_0^\top e^{\lambda_1(t-\tau)}\sqrt{n}\|\hat{\mathbf{z}}(\tau) - \mathbf{z}(\tau)\|d\tau \\ &\leq \|\mathbf{V}(\boldsymbol{\lambda})\boldsymbol{\xi}(0)\| + \int_0^\top e^{\lambda_1(t-\tau)}\sqrt{n}\|\boldsymbol{\xi}(\tau)\|^\delta d\tau.\end{aligned} \tag{A.34}$$

Finally, the proof is completed by using the same arguments as in Theorem 2 of [3]. □

Using similar generalizations, we can also extend Corollary 2 of [3]. More precisely:

Corollary A.1 (Extension of Corollary 2)**.** *The estimation error for the observer* (A.24) *converges exponentially to zero if*

(i) $\begin{bmatrix} L_{\mathbf{f}}^{r_1}h_1(\mathbf{\Phi}^{-1}(\mathbf{z})) \\ \vdots \\ L_{\mathbf{f}}^{r_m}h_m(\mathbf{\Phi}^{-1}(\mathbf{z})) \end{bmatrix}$ *and* $\mathbf{U}(\mathbf{\Phi}^{-1}(\mathbf{z}))$ *are locally Lipschitz;*

(ii) there exists a closed bounded sphere $S(\rho)$ *of radius* ρ *such that* $\mathbf{x}(t) \in S(\rho), \forall \mathbf{u} \in U$

(iii) $\mathbf{Q}(\mathbf{x})$ *has full rank for all* $\mathbf{x} \in S(radius\{(\mathbf{\Phi}^{-1}(S(Nr+r))\})$ *where* $N > 1$ *is an arbitrarily fixed constant and* r *is such that* $\|\mathbf{\Phi}(\mathbf{x})\| \leq r$ *for all* $\mathbf{x} \in S(\rho)$

(iv) $\|\hat{\mathbf{x}}(0) - \mathbf{x}(0)\| \leq \Psi$ *for a suitable* $\Psi > 0$

Proof. The proof is exactly as in Corollary 1, see [3], observing that also the Lipschitz property for $\mathbf{U}(\mathbf{\Phi}^{-1}(\mathbf{z}))$ is guaranteed in $S(radius\{(\mathbf{\Phi}^{-1}(S(Nr+r))\})$. □

A.2 Application to robot manipulator with elastic joints

Consider the dynamical model of a n-dof robot manipulator with joint elasticity as defined in [1]. It can be expressed in state space variables as

$$\begin{aligned}
\dot{\mathbf{x}}_1 &= \mathbf{x}_2 \\
\dot{\mathbf{x}}_2 &= -\mathbf{M}(\mathbf{x}_1)^{-1}\left[\mathbf{c}(\mathbf{x}_1, \mathbf{x}_2) + \mathbf{g}(\mathbf{x}_1) + \mathbf{K}(\mathbf{x}_1 - \mathbf{x}_3)\right] \\
\dot{\mathbf{x}}_3 &= \mathbf{x}_4 \\
\dot{\mathbf{x}}_4 &= \mathbf{J}^{-1}\mathbf{K}(\mathbf{x}_1 - \mathbf{x}_3) + \mathbf{J}^{-1}\mathbf{u}
\end{aligned} \tag{A.35}$$

where the state is $\mathbf{x} \triangleq \begin{bmatrix}\mathbf{x}_1^\top & \mathbf{x}_2^\top & \mathbf{x}_3^\top & \mathbf{x}_4^\top\end{bmatrix}^\top = \begin{bmatrix}\mathbf{q}_1^\top & \dot{\mathbf{q}}_1^\top & \mathbf{q}_2^\top & \dot{\mathbf{q}}_2^\top\end{bmatrix}^\top \in \mathbb{R}^{4n}$.

Claim A.1. *The vector relative degree for the system* (A.35) *with output* $\mathbf{y} \triangleq \mathbf{x}_1 = \mathbf{q}_1 \in \mathbb{R}^n$ *is*

$$\mathbf{r} = \begin{bmatrix} r_1 & r_2 & \cdots & r_n \end{bmatrix}^\top = \begin{bmatrix} 4 & 4 & \cdots & 4 \end{bmatrix}^\top \tag{A.36}$$

Thus $r_1 + r_2 + \cdots + r_n = 4n$.

Proof. Since the i-th component of the vector relative degree represents the first order of derivative of the i-th output which depends on the control, to prove the claim let us compute the derivatives of the output.

$$\begin{aligned}
\dot{\mathbf{y}} &= \dot{\mathbf{x}}_1 = \mathbf{x}_2 \implies r_i \geq 2 && \forall i = 1, \ldots, n \\
\ddot{\mathbf{y}} &= \dot{\mathbf{x}}_2 = -\mathbf{M}(\mathbf{x}_1)^{-1}\left[\mathbf{c}(\mathbf{x}_1, \mathbf{x}_2) + \mathbf{g}(\mathbf{x}_1) + \mathbf{K}(\mathbf{x}_1 - \mathbf{x}_3)\right] \implies r_i \geq 3 && \forall i = 1, \ldots, n \\
\dddot{\mathbf{y}} &= \ddot{\mathbf{x}}_2 = -\frac{\mathrm{d}\mathbf{M}(\mathbf{x}_1)^{-1}}{\mathrm{d}t}\left[\mathbf{c}(\mathbf{x}_1, \mathbf{x}_2) + \mathbf{g}(\mathbf{x}_1) + \mathbf{K}(\mathbf{x}_1 - \mathbf{x}_3)\right] \\
&\quad - \mathbf{M}(\mathbf{x}_1)^{-1}\left\{\frac{\partial(\mathbf{c}(\mathbf{x}_1, \mathbf{x}_2) + \mathbf{g}(\mathbf{x}_1))}{\partial \mathbf{x}_1}\mathbf{x}_2 + \frac{\partial c}{\partial \mathbf{x}_2}\dot{\mathbf{x}}_2 + \mathbf{K}(\mathbf{x}_2 - \mathbf{x}_4)\right\} \\
&= \mathbf{f}_4(\mathbf{x}_1, \mathbf{x}_2, \mathbf{x}_3) + \mathbf{M}(\mathbf{x}_1)^{-1}\mathbf{K}\mathbf{x}_4 \implies r_i \geq 4 && \forall i = 1, \ldots, n \\
\ddddot{\mathbf{y}} &= \frac{\mathrm{d}\mathbf{f}_4(\mathbf{x}_1, \mathbf{x}_2, \mathbf{x}_3)}{\mathrm{d}t} + \frac{\mathrm{d}\mathbf{M}(\mathbf{x}_1)^{-1}}{\mathrm{d}t}\mathbf{K}\mathbf{x}_4 + \mathbf{D}(\mathbf{x}_1)^{-1}\mathbf{K}\dot{\mathbf{x}}_4 \\
&= \mathbf{F}(\mathbf{x}_1, \mathbf{x}_2, \mathbf{x}_3, \mathbf{x}_4) + \mathbf{M}(\mathbf{x}_1)^{-1}\mathbf{K}\mathbf{J}^{-1}\mathbf{u} \implies r_i = 4 && \forall i = 1, \ldots, n
\end{aligned} \tag{A.37}$$

The proof follows immediatly. □

Claim A.2. *Let* $\mathbf{Q}(\mathbf{x})$ *be the matrix defined accordingly to* (A.2) *for the system* (A.35) *with*

output $\mathbf{y} \triangleq \mathbf{x}_1 \in \mathbb{R}^n$*:*

$$\mathbf{Q}(\mathbf{x}) = \frac{\mathrm{d}}{\mathrm{d}\mathbf{x}} \left[\begin{array}{c} x_1^{(1)} \\ L_f x_1^{(1)} \\ L_f^2 x_1^{(1)} \\ L_f^3 x_1^{(1)} \\ \hline \vdots \\ \hline x_1^{(n)} \\ L_f x_1^{(n)} \\ L_f^2 x_1^{(n)} \\ L_f^3 x_1^{(n)} \end{array}\right], \tag{A.38}$$

where $x_1^{(i)}$ *denotes the* i*-th component of* $\mathbf{x}_1$*.* $\mathbf{Q}(\mathbf{x})$ *is nonsingular for any* $\mathbf{x} \in \mathbb{R}^{4n}$*.*

Proof. To prove the result we can show the nonsingularity of any matrix which results from the exchange of the rows of the matrix $\mathbf{Q}(\mathbf{x})$. Let us consider the following matrix $M(\mathbf{x})$,obtained from a suitable reordering of the rows of $\mathbf{Q}(\mathbf{x})$

$$\mathbf{D}(\mathbf{x}) = \frac{\mathrm{d}}{\mathrm{d}\mathbf{x}} \begin{bmatrix} \mathbf{x}_1 \\ L_f \mathbf{x}_1 \\ L_f^2 \mathbf{x}_1 \\ L_f^3 \mathbf{x}_1 \end{bmatrix} = \frac{\mathrm{d}}{\mathrm{d}\mathbf{x}} \begin{bmatrix} \mathbf{y} \\ \dot{\mathbf{y}} \\ \ddot{\mathbf{y}} \\ \dddot{\mathbf{y}} \end{bmatrix} \tag{A.39}$$

In virtute of (A.37), $\mathbf{D}(\mathbf{x})$ is

$$\mathbf{D}(\mathbf{x}) = \begin{bmatrix} \mathbf{I}_n & 0 & 0 & 0 \\ 0 & \mathbf{I}_n & 0 & 0 \\ * & * & -\mathbf{K} & 0 \\ * & * & * & \mathbf{M}(\mathbf{x}_1)^{-1}\mathbf{K} \end{bmatrix} \tag{A.40}$$

Since $\mathbf{M}(\mathbf{x}_1)$ and $\mathbf{K}$ are always invertible, $\mathbf{D}(\mathbf{x})$ is non singular and thus also $\mathbf{Q}(\mathbf{x})$. □

Claim A.3. *The vector*

$$L_f^4 \mathbf{H}\Big|_{\mathbf{x}=\Phi^{-1}(\mathbf{z})} = \begin{bmatrix} L_f^4 x_1^{(1)} \\ \vdots \\ L_f^4 x_1^{(n)} \end{bmatrix}\Bigg|_{\mathbf{x}=\Phi^{-1}(\mathbf{z})} \tag{A.41}$$

is locally Lipschitz.

Proof. $L_f^4 \mathbf{H}\Big|_{\mathbf{x}=\Phi^{-1}(\mathbf{z})}$ is locally Lipschitz since its components are combination of linear, quadratic and sinusoidal functions. □

Claim A.4. *The decoupling matrix*

$$\mathbf{U}(\mathbf{x})\Big|_{\mathbf{x}=\Phi^{-1}(\mathbf{z})} \tag{A.42}$$

is a locally Lipschitz map.

Proof. From (A.37) we have

$$\mathbf{U}(\mathbf{x})\Big|_{\mathbf{x}=\Phi^{-1}(\mathbf{z})} = \mathbf{M}(\mathbf{y}_1)^{-1}\mathbf{K}\mathbf{J}^{-1} \tag{A.43}$$

By the properties of the inertia matrix the claim follows. □

In view of the above claims and the extension of corollary 2 we conclude that is possible to build an observer of the form (3.10) for a generic robot manipulator with elastic joints, choosing as output only the links' positions. In addition, mantaining the same matrix $\mathbf{Q}(\mathbf{x})$ and modifying only $\mathbf{K}$ one can build an observer which uses also the links' velocities.

Claim A.5. *The vector relative degree for the system (2.8) - (2.11) with output*

$$\mathbf{y} \triangleq \begin{bmatrix}\mathbf{x}_3^\top & (\mathbf{K}(\mathbf{x}_1 - \mathbf{x}_3))^\top\end{bmatrix}^\top, \tag{A.44}$$

$\mathbf{y} \in \mathbb{R}^{2n}$*, is:*

$$\mathbf{r} = \begin{bmatrix} r_1 & r_2 & \cdots & r_n & r_{n+1} & \cdots & r_{2n}\end{bmatrix}^\top = \begin{bmatrix} 2 & 2 & \cdots & 2 & 2 & \cdots & 2\end{bmatrix}^\top \tag{A.45}$$

Thus $r_1 + r_2 + \cdots + r_n + r_{n+1} + \cdots + r_{2n} = 4n$.

Proof. The proof works exactly in the same as the one for claim A.1, indeed differentiating twice $\mathbf{y}$ one can see appearing the input $\mathbf{u}$. □

Claim A.6. *The vector relative degree for the system (2.8) - (2.11) with output*

$$\mathbf{y} \triangleq \begin{bmatrix}\mathbf{x}_3^\top & \ddot{\mathbf{x}}_1^\top\end{bmatrix}^\top,$$

$\mathbf{y} \in \mathbb{R}^{2n}$ *is:*

$$\mathbf{r} = \begin{bmatrix} r_1 & r_2 & \cdots & r_n & r_{n+1} & \cdots & r_{2n}\end{bmatrix}^\top = \begin{bmatrix} 2 & 2 & \cdots & 2 & 2 & \cdots & 2\end{bmatrix}^\top \tag{A.46}$$

Thus $r_1 + r_2 + \cdots + r_n + r_{n+1} + \cdots + r_{2n} = 4n$.

Proof. The proof works exactly in the same as the one for claim A.1, indeed differentiating twice $\mathbf{y}$ one can see appearing the input $\mathbf{u}$. □

References

[1] M. W. Spong, "Modeling and Control of Elastic Joint Robots," *Journal of Dynamic Systems, Measurement, and Control*, vol. 109, pp. 310–318, 12 1987.

[2] P. Tomei, "An observer for flexible joint robots," *IEEE Transactions on Automatic Control*, vol. 35, no. 6, pp. 739–743, 1990.

[3] G. Ciccarella, M. D. Mora, and A. Germani, "A luenberger-like observer for nonlinear systems," *International Journal of Control*, vol. 57, no. 3, pp. 537–556, 1993.

[4] A. Isidori, *Nonlinear Control Systems*. Berlin, Heidelberg: Springer-Verlag, 3rd ed., 1995.

[5] A. De Luca, D. Schroder, and M. Thummel, "An acceleration-based state observer for robot manipulators with elastic joints," in *Proceedings 2007 IEEE International Conference on Robotics and Automation*, pp. 3817–3823, 2007.